

GEOTECHNICAL MODELLING OF  
ICEBERG-SEABED INTERACTION

CENTRE FOR NEWFOUNDLAND STUDIES

**TOTAL OF 10 PAGES ONLY  
MAY BE XEROXED**

*(Without Author's Permission)*

HERBERT PAUL GREEN







GEOTECHNICAL MODELLING OF ICEBERG-SEABED INTERACTION

By

Herbert Paul Green, B.Eng., P.Eng.

A thesis submitted to the School of Graduate  
Studies in partial fulfillment of the  
requirements for the degree of  
Master of Engineering

Faculty of Engineering and Applied Science

Memorial University of Newfoundland

May 1984

St. John's

Newfoundland

Canada

### ABSTRACT

Exploratory drilling on the eastern Canadian continental shelf has proven the presence of commercially viable quantities of hydrocarbons. Any process to extract the resources from beneath the seafloor offshore Newfoundland and Labrador has to take into account the severe environmental conditions some of which are unique to this geographic region. Damage to seafloor installations such as pipelines or wellheads by bottom dragging or scouring icebergs is one of the potential problems. This has been recognized since the early 1970's. However, methods of estimating the maximum iceberg scour depths and methods of protecting seabed installations are still topics of research.

In this thesis an experimental approach was taken to physically model the iceberg scour process in a 14 m x 3 m x 1 m towing tank. Cohesionless soil at a uniform slope and with controlled properties was used as the representative seafloor material. Iceberg models 500 mm wide and a pipeline model 122 mm diameter were instrumented and used in a test programme aimed primarily at examining the interaction of the iceberg model and the soil and delineating the influence of the scour process below the incision depth.

For a horizontally scouring iceberg the frontal soil resistance was found to be the major factor affecting

the scour size. The shape of the iceberg keel in contact with the soil was also found to be an important parameter in the scour process. The tests indicate that the zone of soil disturbance extends below the keel of the scouring iceberg. This zone of influence should be accounted for in the design of all buried installations in the Newfoundland and Labrador offshore region.

## KEY WORDS:

Iceberg scour, Canadian continental shelf, geotechnical modelling, marine pipelines, offshore exploration and production, soil pressures, seafloor sediments

---



#### ACKNOWLEDGEMENTS

This thesis was completed at Memorial University of Newfoundland as part of the Ocean Engineering Research program within the Faculty of Engineering and Applied Science. The work was funded by a strategic grant G-0334 from the Natural Sciences and Engineering Research Council of Canada. The author gratefully acknowledges the receipt of a fellowship during the tenure of this work.

The writer is indebted to Dr. T.R. Chari, Associate Dean, Faculty of Engineering and Applied Science for his advice and guidance during the progress of this study. Gratitude is also hereby expressed to the Faculty Technical Staff and the Technical Services Staff for their cooperation and help in the preparation of the experiments. Many thanks are also due to Miss Brenda Young and Mrs. Marilyn Warren for their patient typing of this thesis.

## TABLE OF CONTENTS

	Page
ABSTRACT	ii
KEY WORDS	iv
ACKNOWLEDGEMENTS	v
LIST OF TABLES	ix
LIST OF FIGURES	x
NOTATIONS	xiv
CHAPTER I INTRODUCTION	
1.1 General	1
1.2 Scope of the Work	2
CHAPTER II REVIEW OF LITERATURE	
2.1 General	4
2.2 Icebergs	8
2.2.1 Origin, shapes, sizes	8
2.2.2 Physical properties	14
2.2.3 Iceberg drift	15
2.3 Seabed: Eastern Canadian Continental Shelf	16
2.3.1 Bathymetry	16
2.3.2 Geotechnical properties of the sediments	18
2.3.3 Sediment stability and bottom processes	26
2.4 Iceberg Scour Studies	27
2.4.1 Side scan sonar observations	28
2.4.2 Estimating scour depth	32

	Page
2.5 Iceberg Scour Models	33
2.5.1 Chafi's model	33
2.5.2 Fenco's model	38
2.5.3 Other models	42
CHAPTER III OBJECTIVES OF THE EXPERIMENTS	43
CHAPTER IV EQUIPMENT AND EXPERIMENTAL PROCEDURES	
4.1 Description of Apparatus	46
4.1.1 Towing tank	46
4.1.2 Soil properties	50
4.1.3 Iceberg models	53
4.1.4 Pipeline model	62
4.1.5 Instrumentation	65
4.2 Preparation of the Soil Test Bed	68
4.3 Experimental Procedure	71
CHAPTER V EXPERIMENTAL RESULTS AND DISCUSSION	
5.1 General	79
5.2 Tests on Iceberg Models	80
5.2.1 Iceberg scour profile	80
5.2.2 Soil resistance on iceberg model LI	83
5.2.3 Effect of friction	93
5.2.4 Theoretical computation of soil resistance	100
5.2.5 Effect of towing speed	109
5.2.6 Influence of iceberg model size	111

	Page
5.2.7 Effect of keel shape on the scour process	112
5.3 Tests on the Pipeline Model	118
5.3.1 General	118
5.3.2 Results of tests on the pipeline model	121
5.3.3 Soil pressure away from the centre line of scour	140
5.3.4 Results of tests with the pipeline model in the scour zone	140
5.3.5 Effect of iceberg keel shape on results of the pipeline tests	142
CHAPTER VI SUMMARY AND CONCLUSIONS	146
BIBLIOGRAPHY	150
APPENDIX A Specifications and Calibration Procedures for the Load and Pressure Transducers	158
APPENDIX B Typical Data Sheets for a Scour Experiment	163

LIST OF TABLES

Table		Page
1	ICEBERG CLASSIFICATION BY SIZE (MURRAY 1969)	12
2	ICEBERG CLASSIFICATION BY SHAPE (MURRAY 1969)	13
3	GEO TECHNICAL PROPERTIES OF PISTON CORES FROM DAVIS STRAIT	25
4	SUMMARY OF UNDERWATER CABLES DAMAGED BY ICEBERGS	29
5	ICEBERG SCOUR SIZE COMPUTED FROM CHARI'S MODEL	39
6	ICEBERG SCOUR SIZE COMPUTED FROM FENCO MODEL	41
7	PROPERTIES OF SOIL USED IN THE LABORATORY TESTS	51
8	EFFECT OF FRICTION ON TOTAL LOAD FOR ICEBERG MODEL L1	101

LIST OF FIGURES

Figure		Page
1	GENERALIZED CONCEPTS OF THE ICEBERG SCOUR PROCESS (CHARI ET AL. 1980)	7
2	CURRENT REGIME IN THE NORTH ATLANTIC OCEAN (NEUMANN AND PETERSON 1966)	9
3	ANNUAL NUMBER OF ICEBERGS DETECTED SOUTH OF LATITUDE 48°N (INTERNATIONAL ICE PATROL)	10
4	GENERAL BATHYMETRY OF THE CANADIAN EAST COAST CONTINENTAL SHELF	17
5	LOG OF TWO PISTON CORES FROM NOTRE DAME BAY CHANNEL, NEWFOUNDLAND (MUDIE AND GUILBAULT 1982)	20
6	BOREHOLE LOCATIONS, GRAND BANKS, NEWFOUNDLAND	23
7	IDEALIZED THEORETICAL CONCEPT OF ICEBERG SCOUR MODEL (CHARI 1979)	25
8	COMPUTED AND MEASURED TOTAL PULL ON THE IDEALIZED BERG MODEL (CHARI 1975)	44
9	PLAN AND CROSS-SECTION OF THE TOWING TANK	47
10	CALIBRATION CURVE FOR THE TOWING CARRIAGE	49
11	GRAIN SIZE DISTRIBUTION CURVE FOR THE SOIL USED IN THE TESTS	52
12	SIZES, SHAPES AND IDENTIFIERS OF THE ICEBERG MODELS USED IN THE EXPERIMENTS	54
13	SURFACE ROUGHNESS OF THE ALUMINUM USED FOR THE ICEBERG MODELS	56
14	SOIL-ALUMINUM FRICTION (60 mm SHEAR BOX TESTS)	57
15	SHEAR ENVELOPE: SOIL-ALUMINUM SKIN FRICTION TESTS	58

Figure		Page
16	MOUNTING FRAME FOR ICEBERG MODELS L1 and L2	60
17	MOUNTING FRAME FOR ICEBERG MODELS S1, S2, S3, and L3	61
18	DETAILS OF THE PIPELINE MODEL	63
19	PHOTOGRAPH OF THE PIPELINE MODEL AFTER AN EXPERIMENT	64
20	FLOWCHART OF THE INSTRUMENTATION USED FOR THE ICEBERG SCOUR EXPERIMENTS	66
21	THE RAKE SYSTEM FOR SOIL TEST BED PREPARATION	70
22	AN EXPERIMENT IN PROGRESS WITH ICEBERG MODEL L1	73
23	SOIL TEST BED AFTER A SCOUR EXPERIMENT	74
24	DETAILS OF THE EQUIPMENT FOR MEASURING IN SITU PROPERTIES OF THE SOIL TEST BED	76
25	PROFILE OF SCOUR CROSS-SECTION PERPENDICULAR TO THE SCOUR LENGTH	81
26	TYPICAL HORIZONTAL FORCE RECORD FOR ICEBERG MODEL L1	85
27	SOIL FAILURE ALONG SUCCESSIVE SHEAR PLANES IN FRONT OF EARTHMOVING MACHINES (SIEMENS 1963)	87
28	SUCCESSIVE FAILURE PLANES IN FRONT OF ICEBERG MODEL L1	88
29	TOTAL HORIZONTAL FORCE MEASURED ON ICEBERG MODEL L1	90
30	TYPICAL RESULTS OF SOIL PRESSURE MEASURED ON THE FRONT FACE OF ICEBERG MODEL L1	91
31	VARIATION OF SOIL PRESSURE ON THE FRONT FACE OF MODEL L1	92
32	COMPARISON OF THE TOTAL MEASURED LOAD ON ICEBERG MODEL L1 WITH THE LOAD ON THE FRONT FACE	94

Figure		Page
33	INFLUENCE OF FRICTION ON THEORETICAL SCOUR DEPTHS (CHARI AND GREEN 1981)	95
34	COMPARISON OF SOIL PRESSURE ON THE FRONT AND SIDE OF MODEL L1, 40 mm ABOVE THE BASE	97
35	COMPARISON OF SOIL PRESSURE ON THE FRONT AND SIDE OF MODEL L1, 190 mm ABOVE THE BASE	98
36	COMPARISON OF SOIL PRESSURE ON THE FRONT AND BASE OF MODEL L1	99
37	COMPARISON OF THE MEASURED TOTAL SOIL RESISTANCE ON ICEBERG MODEL L1 WITH THE FRONT, SIDE AND BASE COMPONENTS OF SOIL RESISTANCE	102
38	MEASURED HEIGHT AND LENGTH OF SURCHARGE FOR ICEBERG MODEL L1 THE SCOUR LENGTH	104
39	COMPARISON OF MEASURED AND THEORETICAL TOTAL FORCE ON ICEBERG MODEL L1	105
40	RESULTS OF THE EXPERIMENT WITH PRESSURE TRANSDUCERS INSIDE THE SOIL (CHARI 1975)	107
41	CONCEPTUAL SOIL MOVEMENT IN FRONT OF THE IDEALIZED ICEBERG (CHARI 1975)	108
42	EFFECT OF ICEBERG MODEL SPEED ON MEASURED LOAD FOR MODEL L1	110
43	COMPARISON OF LOAD MEASURED ON ICEBERG MODELS L3 AND S3	113
44	COMPARISON OF LOAD MEASURED ON ICEBERG MODELS L1 AND L2	115
45	VARIATION OF SOIL PRESSURE ON THE FRONT FACE OF MODEL L2	116
46	COMPARISON OF SOIL PRESSURES MEASURED ON THE EIGHT SIDES OF THE PIPELINE MODEL	120
47	LOCATIONS OF THE PIPELINE MODEL IN THE SOIL TEST BED FOR THE EXPERIMENTS WITH ICEBERG MODEL L1	122

Figure		Page
48	PIPELINE RESULTS, MODEL L1, A, STATION 1	123
49	PIPELINE RESULTS, MODEL L1, A, STATION 2	124
50	PIPELINE RESULTS, MODEL L1, A, STATION 3	125
51	PIPELINE RESULTS, MODEL L1, B, STATION 1	126
52	PIPELINE RESULTS, MODEL L1, B, STATION 2	127
53	PIPELINE RESULTS, MODEL L1, B, STATION 3	128
54	PIPELINE RESULTS, MODEL L1, C, STATION 1	129
55	PIPELINE RESULTS, MODEL L1, C, STATION 2	130
56	PIPELINE RESULTS, MODEL L1, C, STATION 3	131
57	MAXIMUM MEASURED PRESSURES ON FACE A OF THE PIPELINE MODEL	134
58	MAXIMUM MEASURED PRESSURES ON FACE B OF THE PIPELINE MODEL	135
59	MAXIMUM MEASURED PRESSURES ON FACE C OF THE PIPELINE MODEL	136
60	COMPARISON OF THEORETICAL AND MEASURED PRESSURES (CHARI ET AL. 1982)	137
61	REDUCTION OF PRESSURE WITH INCREASING DEPTH OF PIPELINE BURIAL BELOW THE SCOUR (CHARI ET AL. 1982)	139
62	PIPELINE RESULTS, MODEL L1, LATERAL VARIATION OF PRESSURE ON THE PIPE	141
63	PIPELINE RESULTS, MODEL L1, TOP OF PIPE 47 mm ABOVE MAXIMUM DEPTH OF SCOUR	143
64	PIPELINE RESULTS, MODEL L1, TOP OF PIPE 132 mm ABOVE MAXIMUM DEPTH OF SCOUR	144
65	COMPARISON OF PRESSURE ON THE PIPELINE MODEL FOR ICEBERG MODELS L1 AND L2	145

NOTATIONS

The symbols used in this thesis and identified below are in accordance with the recommendations published in the Canadian Geotechnical Journal (Barsvary et al. 1980).

The symbols are defined when they first appear in the text.

A	projected area of a submerged iceberg normal to the propelling current
B	width of the idealized iceberg, also width of the scour
c	cohesion
$C_d$	drag coefficient
$C_u$	uniformity coefficient
d	scour depth at any instant during scouring
$d_p$	depth from bottom of scour to top of pipeline model
D	maximum depth of scour
E	modulus of elasticity
$F_d$	drag force on a decelerating iceberg
g	acceleration due to gravity
h	height of surcharged soil in front at any instant during scouring
H	final height of the surcharged soil
$I_L$	liquidity index
K	subgrade modulus
l	length of scour at any instant during scouring
L	maximum length of scour
P	soil resistance on the front face of the idealized iceberg

t	time
V	initial steady state velocity of the iceberg and current velocity
W	weight of the iceberg
$w_p$	plastic limit
$w_l$	liquid limit
w	natural water content of a sediment
$\alpha$	angle of slope of displaced soil
$\beta$	angle of slope of seafloor
$\delta$	angle of friction between iceberg model and soil
$\gamma'$	submerged unit weight of soil
$\gamma_{sat}$	saturated unit weight of soil
$\gamma_{max}$	maximum dry unit weight of the soil used in the tests
$\gamma_{min}$	minimum dry unit weight of the soil used in the tests
$\gamma_{exp}$	actual unit weight of the soil as used in the test
$\phi$	$\pi/4 - \psi/2$
$\tau$	undrained shear strength of the soil
$\phi$	angle of internal friction (total)
$\nu$	Poisson's ratio

## CHAPTER I

### INTRODUCTION

#### 1.1 General

Offshore activity worldwide has increased dramatically in the last two decades. This has come about mainly as a result of an increasing need to harvest the resources beneath the sea. As the reserves of minerals and hydrocarbons on land become more expensive to explore and extract, the alternative of obtaining these from the seabed is becoming more feasible. Canada, with its vast coastal regions is a prime example of a country experiencing a healthy growth in its offshore petroleum industry. The main areas of interest at present are the Canadian Arctic and the Canadian East Coast continental shelf.

Large reserves of hydrocarbons have been proven offshore Newfoundland and Nova Scotia. Further north, off Labrador and in the Davis Strait a continuing exploration program has yielded promising results. The eventual goal is the safe and orderly development of these resources. Achieving this goal requires an understanding of the possible engineering problems and their solutions. One particular hazard unique to the Canadian East Coast is the seasonal presence of icebergs. The iceberg threat is twofold; the possibility of a direct impact with an offshore drilling platform and the scouring of the ocean floor by a bottom

dragging iceberg. Iceberg scours as deep as 6.5 m and several kilometers long have been measured on the continental shelf (Harris and Jollymore 1974). Scouring icebergs could dislodge and uproot any bottom structure such as pipelines or wellheads in the zone of scour. The implications of this phenomenon on offshore development along the Canadian East Coast was recognized in the early 1970's (Allen 1971). Engineering analysis of the iceberg scour problem is one of the ongoing research activities at Memorial University of Newfoundland. Some aspects of iceberg scouring in relation to the safe burial depths of pipelines in the East Coast waters are examined in this thesis.

## 1.2 Scope of the Work

Studies on iceberg scours were initiated by the Ocean Engineering Research group at Memorial University of Newfoundland in the early 1970's as part of its mandate to address the problems of concern to the Canadian offshore industry. A preliminary theory of iceberg grounding was proposed by Chari and Allen (1972). Refinements of the original theory and experimental verification through physical modelling of the scour process for clay soils were subsequently completed (Chari 1975). A comprehensive summary of completed work and suggestions for further research were given by Chari (1979). An extension of this work to cohesionless soils and its application to the design of safe

burial depths for seabed installations are reported in this thesis. This research is part of a continuing programme at Memorial University to try and understand the iceberg scour phenomenon and to optimize solutions to cope with the problem. The results reported here pertain to physical modelling and laboratory experiments.

The presentation in this thesis has been organized into six main chapters. Chapter II is a review of the literature related to icebergs, the Canadian eastern continental shelf, geotechnical properties of marine sediments, field data on scours, iceberg scour models and applicable soil mechanics theories and methods.

Chapter III explains the aims and objectives of the physical models used in this research. Chapter IV contains a description of the laboratory facilities, the types of experiments conducted and the instrumentation. The objective of the experiments was to investigate the interaction at the iceberg-soil boundary by using physical models which were larger than those used earlier.

Chapter V contains the compilation and presentation of experimental results as well as an analysis of the experimental data. Practical applications of the results of this work to the oceans are also examined and discussed in Chapter V.

Chapter VI summarizes the conclusions and contains suggestions for further work.

## CHAPTER II

### REVIEW OF LITERATURE

#### 2.1 General

In engineering, and in particular in civil engineering, the term "scour" is often used to describe the erosion or winnowing away of surficial sediments due to hydrodynamic effects around structures such as bridge piers or offshore platforms. Geologists have used the same term for the ploughed features left on land and on the seabed by receding glaciers and icebergs (Lewis et al. 1979; Dredge 1982). As opposed to the conventional civil engineering "scour", iceberg scours are long trough-like features usually characterized by raised shoulders on both sides and a valley-like form in between. There are several terms used in the literature to describe the same phenomenon; microrelief (Carsola 1954), scores (Kovacs 1972), furrows (Harris and Jollymore 1974), gouges (Barnes et al. 1982). The nomenclature "scour" is now generally accepted as the standard terminology by the scientific and engineering communities in Canada to include all the above terms (NRCC Workshop 1982). These scours have been observed and measured in the Beaufort Sea, in the Great Lakes and on the continental shelf off the Canadian East Coast. In the Beaufort Sea and in the Great Lakes, ice keels grounding in

shallow water cause the scour, while on the Canadian East Coast the scours are primarily due to icebergs. Although the scour features are similar in all three locations, the type of environmental driving forces causing the scour are somewhat different in each case.

A scour may be produced when an ice feature drifts to an area where the water depth is less than the draft of the ice keel. The type of iceberg-seabed interaction depends on a number of physical parameters which will be discussed later. Besides scours, pock marks have been observed on the seafloor off the Canadian East Coast (Fader and King 1981). Pock marks are circular or elliptical depressions or pits on the seabed and are found in several locations across the oceans. One suspected reason for the formation of pock marks especially in areas where icebergs are not common is the release of shallow deposits of gas from the seabed and the consequent slumping of the sediments (Esrig and Kirby 1977; Hovland 1983). However on the continental shelf off Eastern Canada the origin of the pock marks has not been well established. They may be attributed to icebergs squatting on the seafloor possibly due to tidal fluctuations or due to a stopping of the iceberg and grounding at the end of a scour (Lewis and Barrie 1981). Long scour tracks are a greater hazard than pock marks on the Canadian continental shelf.

Icebergs are generally very large and it has been reported (Milne 1973) that instruments located on the seabed in 500 m water in Baffin Bay were damaged by grounding icebergs. Icebergs will float and generally drift under the action of ocean currents as long as the water is deeper than the draft of the iceberg. When an iceberg comes to a location where the water depth is shallower than the iceberg draft, it will first touch and then drag along the bottom to form a scour. Conceptually, iceberg scouring can be visualized as shown in Fig. 1 (Chari et al. 1980). If the ocean floor is hard such as a rock outcrop, the grounding iceberg will travel up slope without forming a distinct and visible scour mark. This is shown in Case A of Fig. 1. If the ocean floor consists of sediments and the soil has adequate bearing capacity to support a part of the berg's weight, the scour phenomenon may be a combination of seabed ploughing by the iceberg combined with a simultaneous uplift, Case B, Fig. 1. A third possibility is the situation when the seabed is weak and soft in which case the iceberg plows the seafloor horizontally with little or no uplift, Case C, Fig. 1. It is thus obvious that parameters such as the iceberg size, its velocity, the seabed type, its geotechnical properties and the bathymetry will influence the scour process.

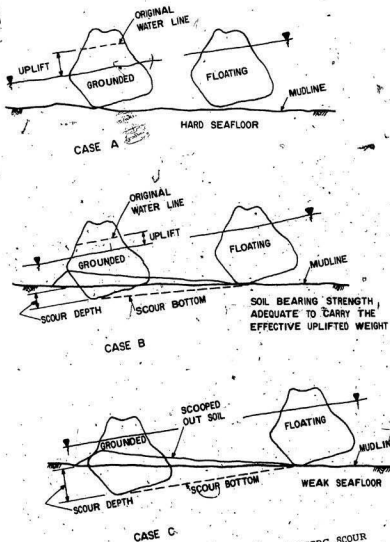


FIG. 1 GENERALIZED CONCEPTS OF THE ICEBERG SCOUR PROCESS (CHARI ET AL. 1980)

## 2.2 Icebergs

While interest in icebergs has increased in recent years, mostly due to increased offshore exploration activities, icebergs have historically been a concern to North Atlantic mariners for many years. Peters (1979) has reviewed the history of iceberg observations and iceberg studies pertaining to the Canadian east coast. Since its formation in 1914, the International Ice Patrol has been regularly studying icebergs. Substantial amounts of scientific data on icebergs were also collected during the Marion expedition (Smith 1931).

### 2.2.1 Origin, shapes and sizes

The principal source of North Atlantic icebergs are the 20 major tidewater glaciers on the west coast of Greenland (Dinsmore 1972). It is estimated that as many as 15,000 icebergs may be calved annually from these glaciers. However, a major portion of these are trapped in the bays and coastal indentations enroute (Fig. 2) where they ultimately disintegrate. Only a small fraction travel all the way to the southerly latitudes. Fig. 3 shows the annual number of icebergs drifting south of latitude 40°N for the period 1900 to 1980. The average value is 378 with a standard deviation of 369 indicating a wide variation in the annual iceberg population.

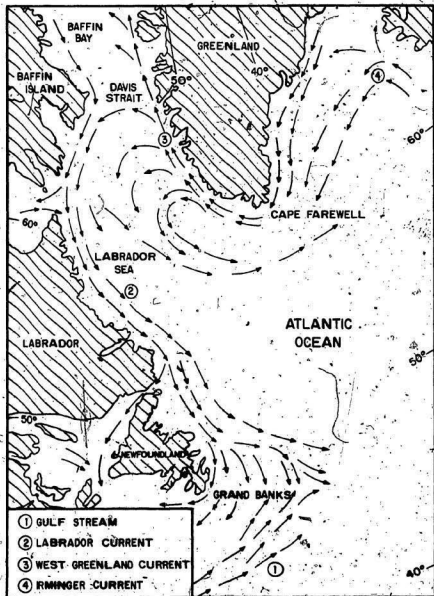


FIG. 2 CURRENT REGIME IN THE NORTH ATLANTIC OCEAN  
(NEUMANN AND PIERSON 1966)

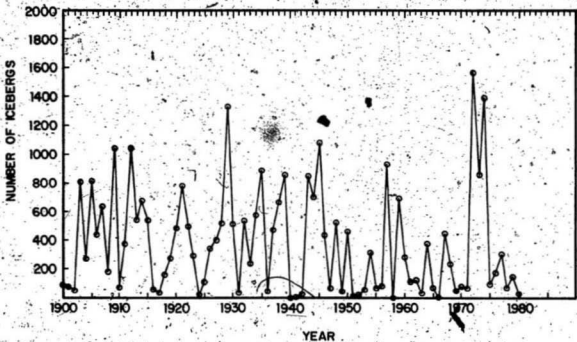


FIG. 3 ANNUAL NUMBER OF ICEBERGS DETECTED SOUTH OF LATITUDE 48°N (INTERNATIONAL ICE PATROL)

Icebergs are usually quite large near the source of formation. Icebergs in excess of 1000 m in length have been reported near the Steenstrup Glacier around Cape York, West Greenland (Kollmeyer 1980). While the icebergs drift in the ocean currents, the process of melting alters their shape and mass. The rate of iceberg melting is dependent on the iceberg composition, sea water temperature, currents, wave action and the weather conditions. Icebergs which are sited along the coast of Newfoundland and Labrador were most probably calved about three years earlier (Binsmore 1972), drifted slowly in the ocean currents and ice fields and have usually undergone a large decrease in mass and subsequent changes in shape during that period, resulting in icebergs of random dimensions. Icebergs are conventionally classified by their above-water shape. The International Ice Patrol uses a classification system based on estimated size and shape (Murray 1969) (Table 1 and 2). The submerged volume of the iceberg will be about seven times the above water volume on the assumption that iceberg ice has the same specific gravity of 0.9 as glacier ice (Embleton and King 1971) and the specific gravity of sea water is 1.03. However the ratio between draft and above-water height will not be in the same proportion and will depend on the shape of the iceberg. Draft to height ratios from 10.56:1 to 1.29:1 have been reported (Benedict 1976). Allaire (1972) calculated draft to

TABLE 1. ICEBERG CLASSIFICATION BY SIZE (MURRAY 1969):

Name	Height		Length	
	m	(ft)	m	(ft)
<b>Tabular berg</b>				
S - small	<6	<20	<91	<300
M - medium	6 to 15	20 to 50	91 to 213	300 to 700
L - large	>15	>50	>213	>700
<b>Others</b>				
S - small	<15	<50	<61	<200
M - medium	15 to 46	50 to 150	61 to 122	200 to 400
L - large	46 to 78	150 to 255	122 to 213	400 to 700
VL - very large	>78	>255	>213	>700

TABLE 2. ICEBERG CLASSIFICATION BY SHAPE (MURRAY 1969)

Type	Description
B - blocky	Steep precipitous sides with horizontal or flat top, very solid berg, length/height ratio 5:1.
DK - drydock	Eroded such that a large U-shaped slot is formed with sharp corners or pinnacles, slot extends into waterline or close to it.
D - dome	Large smooth rounded top, solid type berg.
P - pinnacled	Large central spire or pyramid of one or more spires dominating the shape, less mass than dome shaped bergs of similar dimensions.
T - tabular	Horizontal or flat topped berg with length to height ratio 5:1
Bergy bit	A mass of glacial ice smaller than a berg, but larger than a growler, about the size of a small cottage, small berg or large growler is preferred usage.
Growler	A mass of glacial ice calved from a berg or is the remains of a berg. Less than 2.5 m high and .6 m long.

height ratios of 9:1 to 1:1 for simple idealized berg shapes. It may thus be noticed that the draft of an iceberg, which is an important parameter in the scour process, is highly variable and dependent on a number of factors.

### 2.2.2 Physical properties

One of the assumptions in evaluating the maximum depth of iceberg scours is that the iceberg does not fracture or break up during the interaction with the seabed. Published information on the physical and engineering properties of iceberg ice is limited. Recent tests on samples from a grounded iceberg (Arocklasamy et al. 1983) gave an average density of 0.904 g/cm<sup>3</sup>. Unconfined compression strength was in the range of 4 to 10 MPa and partially confined crushing strength tests simulating berg impact with a semi-submersible gave values in the range of 22 to 38 MPa. The allowable bearing capacity for soils on land ranges from 0.02 MPa for soft clays to about 1.0 MPa for compact sands and gravels (Bowles 1982). It would thus appear that the iceberg has a relatively large strength compared to that of seabed soils which in the extreme may have a shear strength up to 1.0 MPa. The scouring process would thus be somewhat similar to the different cases shown in Fig. 1.

### 2.2.3 Iceberg drift

The velocity of an iceberg and the kinetic energy it has when it touches the seabed at the instant of grounding will influence the length of the scour. The generalized drift pattern of icebergs in the North Atlantic depends largely on the ocean currents (Dinamore 1972) as shown in Fig. 2. After calving, most icebergs drift along the West Greenland and Baffin Island coast where they are caught in the southeasterly flowing Labrador Current. The system of ocean currents in Baffin Bay, Davis Strait and the Labrador Sea is the predominant factor resulting in the southerly movement of icebergs. In the process of their long travel, a number of bergs are trapped in shoreline waters along the way. Icebergs which finally reach the Grand Banks disintegrate in days or weeks under the influence of the warm Gulf Stream. The long-term drift pattern of icebergs has been generally well established over the years by various observation and tracking programmes (Robe et al. 1980).

Another type of iceberg movement, which is the short term drift, is of importance to offshore operators in predicting the risk of a direct impact with stationary objects such as drilling rigs or ships. For this reason drilling vessels are staffed with ice observers to record and predict local ice movement during the ice season. The amount of lead time required to disconnect the drilling well and

move away from the path of an oncoming iceberg will depend on the complexity of the equipment and the weather conditions. The short term iceberg drift depends on the iceberg size and shape, currents in the immediate vicinity of the iceberg, winds, waves, sea level pressure gradients and Coriolis effects (El-Tahan 1980). Estimating these data is a major task in the accurate prediction of iceberg drift (Mountain 1980). Based on the reported observations, it is reasonable to assume maximum drift velocities of 48 km/day for long term drift (Dinsmore 1972) and 1.2 m/sec for short term drift (El-Tahan et al. 1983).

### 2.3 Seabed: Eastern Canadian Continental Shelf

The bathymetry and seabed type are important parameters in the scour process. A soft sediment would be more vulnerable to a deeper scour than a dense sand or gravel. Similarly an iceberg plowing into a steep bank will ground after a short travel while the scour track will be long if the bathymetry is relatively flat. These aspects will be reviewed below.

#### 2.3.1 Bathymetry

A bathymetric chart of the Canadian East Coast is shown in Fig. 4. The outer margin of the continental shelf is generally taken as the 500 m. isobath. In water depths

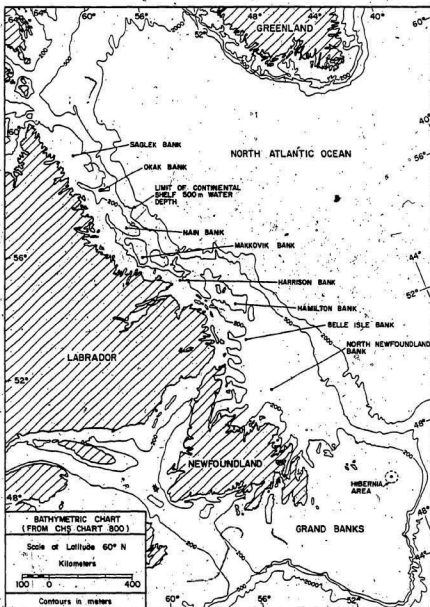


FIG. 4 GENERAL BATHYMETRY OF THE CANADIAN EAST COAST CONTINENTAL SHELF.

greater than 500 m the seabed slope tends to increase quickly with depth, along the continental slope. The 200 m isobath is the limit of interest for iceberg scour considerations. The width of the continental shelf is about 100 to 300 km. Towards the shore a longitudinal channel separates a narrow and rough inner shelf from a smooth wide outer shelf. Transverse troughs divide the outer shelf into a series of discrete bank areas as identified in Fig. 4. The tops of the banks are generally flat with depths between 70 to 200 m (Grant 1972). It is these banks which are of interest to the oil industry as potential areas for oil exploration and these banks are also susceptible to frequent scouring and grounding of icebergs because of the shallow water depths.

### 2.3.2 Geotechnical properties of the sediments

The length and depth of an iceberg scour depends on the resistance of the seabed to the ploughing action of the berg. This resistance is quantified in terms of shear strength and other geotechnical parameters of the seafloor. Geotechnical information for most areas of the Canadian East Coast is sparse. Information on the general types of sediments as obtained from geological and geotechnical sources are presented below.

Litvin and Rvachev (1963) collected data for identifying the seabed type primarily as an aid to improve

the efficiency of trawler techniques. Based on 198 samples it was concluded that the Hamilton Bank and the Grand Banks are mostly composed of sand occasionally mixed with boulders, gravel and mud. Large mud deposits occur on the North Newfoundland Bank and along the slopes of the Hamilton and Grand Banks.

Slatt (1974) classified over 300 grab samples from the Grand Banks and the North Newfoundland Bank. Medium to fine sand with particle sizes from 2 to 0.064 mm were identified on the outer Grand Banks. Landward on the inner Grand Banks, coarse sand and gravel predominate. Silt and clay size sediments were found on the North Newfoundland Bank.

Results of geological analysis have been reported (Mudie and Guilbault 1982) of two piston core samples, 8.5 and 11.0 m long, obtained in 286 m water depth off the northeast coast of Newfoundland (Fig. 5). It is inferred the shear strengths of the sediments is relatively low since the piston corer penetrated 11 m into the seabed.

Van der Linden et al. (1976) summarized seismic and bottom sampling data from the Hamilton Bank. Its perimeter consists of a band of sediment ranging from sand to gravel. Landward, grain size decreases to muddy fine sand and fine sandy mud from 1 to 10 m thick. The adjoining trough areas are composed of silty clays.

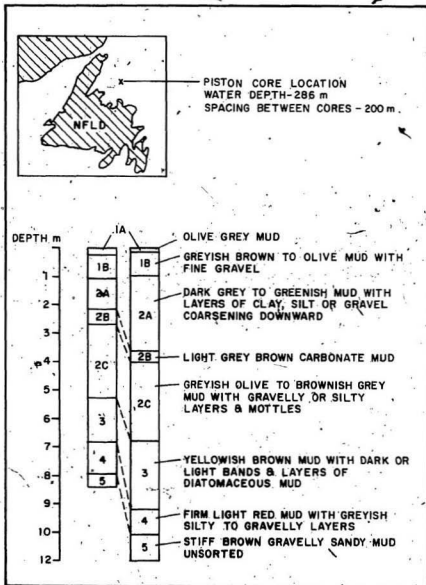


FIG. 5 LOG OF TWO PISTON CORES FROM NOTRE DAME BAY CHANNEL, NEWFOUNDLAND (MUDIE AND GUILBAULT 1982).

Fillon and Harmes (1982) conducted a similar analysis for sediments on the Saglék Bank off northern Labrador. A 0.1 to 2 m layer of mud (less than 10% sand and gravel) covers the bank underlain by soft muds and compacted sediments. Corer penetration varied from 1 to 10 m depending on sediment strength.

Kellor (1969) summarized the analysis of over 300 samples from the North Atlantic, and gave the following range of geotechnical properties for the Canadian East Coast surficial sediments:

Sediment type:	Fluvial-marine (sand-silt sizes greater than 0.016 mm)
Shear strength ( $\tau$ ):	3.4 to 6.9 kPa
Water content (w) :	50 to 100%
Saturated unit wt. ( $\gamma_{sat}$ ):	14.8 to 17.1 kN/m <sup>3</sup>

Fifteen short core samples from the southern Grand Banks area were tested by Geocop (1969). Water depth was approximately 95 m, core lengths ranged from 0.38 to 1.37 m, the average length being 0.80 m. The results of these tests are summarized below:

Location:	44° to 45°N, 52° to 53.5°W
Sediment type:	sand and combinations of sand, silt, gravel
$\gamma_{sat}$ :	14 to 20 kN/m <sup>3</sup>
$\phi$ :	34 to 57° (from direct shear tests on disturbed samples)

A series of three bore holes on the Grand Banks by McClelland Engineers (1971) (Fig. 6) indicated 4 to 26 m of dense sand as the upper layer underlain by hard silts or stiff clays occasionally with sand seams. A value of  $\phi = 35^\circ$  for the sand was suggested which is near the range of values of  $\phi = 39$  to  $46^\circ$  given by Geocon (1969) for their four cores closest (12 to 23 km away) to McClelland's borehole number 3.

Based on the results of three boreholes (Fig. 6) drilled in 1980 (Geocon 1980) in the Hibernia area of the Grand Banks, the upper 5 to 6 m was found to be dense clean sand with traces of gravel, silt, clay and shells. The degree of sediment compaction is apparent due to the reported difficulties in advancing the drilling and in driving 50 mm O.D. sampling tubes and split spoons. The sand was underlain by various strata from silty clay to clayey silt to silty sand. Direct shear tests on reconstituted samples from the upper sand layers gave  $\phi$  values of 36 to  $40^\circ$ .

From the efforts required to obtain vibrocore samples in 70 m water depth at Hibernia, Amos and Barrie

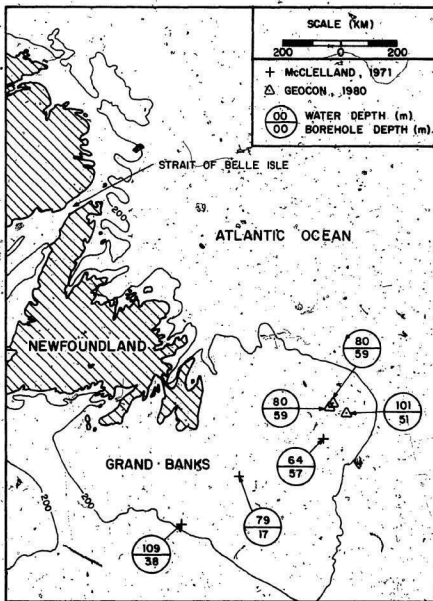


FIG. 6. BOREHOLE LOCATIONS, GRAND BANKS, NEWFOUNDLAND

(1980) concluded that the seabed was hard with lag gravel. Also in the Hibernia area the author participated in tests with a free fall impact penetrometer. Because of the dense nature of the seabed (Lewis 1981) the load cells of the penetrometer failed by buckling. Tests on Van Veen grab samples from these locations showed the following:

Location : Hibernia area, Grand Banks  
 Sediment type: medium to fine sand poorly graded  
 $\gamma_{sat}$ : 19 to 21 kN/m<sup>3</sup>  
 $\phi$ : 27 to 32°

Some geotechnical data is also available for the Davis Strait area (Fig. 2). MacLaren Atlantic Limited (1976) studied two piston cores, in 540 m water depths. Graham and Nixon (1979) discuss the results of tests of 6 cm diameter piston cores from 400 m water depth in the southern Davis Strait. Although these water depths are probably too deep for iceberg scours the geotechnical properties are of general interest and are given in Table 3. Additional geotechnical tests on 10 piston core samples from the Davis Strait in 300 m water depth had the following properties (Chari et al. 1983):

Sediment type: sand & silt mixtures  
 $\gamma_{sat}$ : 20 kN/m<sup>3</sup>  
 $\phi$ : 25° (direct shear tests on reconstituted samples)

TABLE 3 GEOTECHNICAL PROPERTIES OF PISTON CORES FROM DAVIS STRAIT

Parameter	MacLaren (1976)	Graham and Nixon (1979)
Location	Davis Strait	Davis Strait
Water depth	540 m	400 m
Sediment type	Olive grey sand (SM) 5 to 10 cm thk. overlying dark greenish grey mud (CL-MC)	clay (CL) < 40% sand and gravel
Saturated unit weight $\gamma_{sat}$	-	22 kN/m <sup>3</sup>
Water content w	17%	15%
Liquidity index $I_L$	0.10%	0.14 to 0.53
Plastic limit $w_p$	15.9%	-
Liquid limit $w_l$	23.7%	-
Shear strength $\tau$	-	17 to 31 kPa
Cohesion c	-	7 kPa
Angle of Internal Friction $\phi$	-	34°

Results of tests on samples from the Strait of Belle Isle (Fig. 6) during feasibility studies for power cable crossings showed that the soil overburden was of an average thickness of 2.2 m. It is composed of a medium dense to dense layer of sand and gravel with cobbles and boulders overlying a discontinuous stratum of very dense glacial till or bedrock. At some locations soil thickness reached 12 to 18 m (Green et al. 1982). The Strait is in the path of the icebergs, has water depths of 44 to 120 m and is prone to iceberg groundings.

Based on the available geological and geotechnical data for the continental shelf offshore Eastern Canada, it appears that significant areas are composed of sands and gravels, while other areas consist of finer grained sediments. To investigate the scour potential at a given location it would be necessary to examine the surficial sediments in detail at the specific location to a depth of 4 to 5m below the mudline.

### 2.3.3 Sediment stability and bottom processes

An understanding of the dynamics of the continental shelf sediments is important with respect to iceberg scours and with respect to the engineering design of seabed structures. Scour features may be generally altered in course of time by erosion or deposition of material

thereby changing the scour dimensions. Also, bottom processes will influence the geotechnical properties of sediments, which in turn will influence the soil resistance to iceberg scour or its ability to support a structure.

In shallower waters, the effect of the bottom currents and long waves will influence the seabed stability. Field data on both these aspects are somewhat limited at present. It is reported (Lewis and Barrie 1981) that storm generated bottom currents in the Hibernia location are of sufficient intensity to cause intermittent sediment transport. This is based on observations of the seafloor, analysis of sediment grain sizes and current meter measurements. On the Makkevik and Hamilton Banks (Fig. 4) movement of bottom sediments was observed in water depths of 450m (Josenhans and Barrie 1982).

Further field data would be required before any definite conclusions can be drawn on the effect of sediment movement on iceberg scours.

#### 2.4. Iceberg Scour Studies

Damage to seabed fishing gear like lobster pots by icebergs has been a recognized fact by Newfoundland fishermen for a long time. Trans-Atlantic submarine communications cables have been periodically broken by grounding icebergs, although the cables are normally laid

along a circuitous route following bathymetric lows. A summary of the cable breaks along the shelf areas of Greenland and Newfoundland since 1960 is contained in Table 4.

Since 1974 geologists have documented field data on iceberg scours through side scan sonar and shallow seismic surveys. Some of this work is reviewed below.

#### 2.4.1 Side scan sonar observations

The acoustic methods used to map the seafloor are the deep tow, high resolution shallow seismic profiler and the side scan sonar. The seismic profiler is capable of resolution to 0.3 m and penetration to a depth of approximately 75 m (Josenhans 1983) in which the scours appear as U-shaped indentations. The side scan sonar uses a tow fish that projects a fan shaped acoustic beam from both sides. The swath width is about 1.5 km. Reflected echoes are recorded and used to produce a plan view map of the seabed. Bottom irregularities like scours appear as light and dark lines.

Harris (1974) and Harris and Jollymore (1974) observed iceberg scours along the Labrador Shelf in water depths of 155 to 275 m east of Belle Isle (Fig. 4). Scours of average width 30 m, maximum depth 6.5 m and as long as 3 km were measured.

TABLE 4 SUMMARY OF UNDERWATER CABLES DAMAGED BY ICEBERGS

Year	Number of cable breaks	Water depth (m)	Location
*1960	1	366	Northeast of Cape Mercy, Baffin Island, Davis Strait
**1961	1	100	East of Bonavista Peninsula, Newfoundland
*1963-1970	19	77 to 209	Off Cape Farewell, Greenland
*1965-1970	4	190 to 212	South of Thule, Greenland, Baffin Bay

\*Gustajtis (1979)

\*\*Navigation Report C.S. Lord Kelvin (1961).

Van der Linden et al. (1976) discussed iceberg scour data gathered in 1972 and 1973 from the Hamilton Bank. Gouges up to 4 m deep and several kilometers long were measured with orientations generally in the direction of the Labrador Current.

King (1976) reported scours 2 to 3 m deep and 30 to 40 m wide with raised rims in water depths of 105 to 120 m along the Laurentian Channel and western Grand Banks off the south coast of Newfoundland.

Lewis et al. (1979) summarized scour data obtained from Saglek Bank, Labrador to Cape York, Greenland. Bottom features varying from pock marks to long scour tracks, and scours formed by multi-keeled bergs were observed. Widths varied from tens of meters to greater than 100 m, with scour depths in the range of a few meters.

Lewis and Barrie (1981) reported scour features in the Hibernia area of the Grand Banks. Scours as deep as 5.4 m and from 3 to 124 m wide were measured in water depths up to 150 m. Two populations of scours were distinguished. In water depths greater than 110 m, a dense pattern of degraded furrows and pits exist. In water depths of 60 to 160 m fresh looking and less dense patterns of scours were observed. The deepest iceberg scour was 5.4 m although an unconfirmed circular depression 6.5' m deep was noted.

To supplement acoustically sensed scour data, manned submersibles have been used to survey the seabed. Using *Piscés IV* (Josefhans and Barrié 1982) seabed investigations were conducted in the Bjarni wellsite area of Makkovik Bank (water depth less than 200 m) and along the southwest Harrison Bank (water depth 300 to 450 m). Within the near bottom current regime investigated, they suggest that older scour marks can be identified by the lack of a fine matrix within their ridges and the lack of significant relief. Recent scours have well-developed ridges up to 2 m high with ridge slopes of 3 to 6° (measured perpendicular to the length of scour) and are composed of cobbles and boulders protruding slightly from a matrix of silty sand. Attempts to penetrate the seabed with the *Piscés IV* corer were unsuccessful. The subsurface was too coarse in the ridges and too compacted within the scour trough. Another method of relative dating of the scours is by estimating the extent of biological activity on boulders and cobbles in and around the scour. Some ice-rafted boulders were observed to have a dense organic coating, others had a fresh surface indicating more recent deposition.

Other evidence to substantiate iceberg scouring is based on the observations of grounded bergs. Barrié et al. (1982) reported an ongoing project to review iceberg flux and groundings from drill rig iceberg observation records.

from 1973 to 1976. The study area was the eastern Canadian continental shelf from 40°N to 60°N. Out of 800 bergs, 39 grounding events were detected in water depths ranging from 110 to 380 m. The process of iceberg-seabed contact was identified based on the berg's erratic and slow drift velocities. Draft measurements were also made showing some correlation with water depth.

#### 2.4.2 Estimating scour depth

Many of the scours on the Canadian continental shelf are probably relict; however in some areas the process is still quite active (Woodworth-Lynas 1983). Two approaches to determining maximum scour depth may be used. The first involves periodic surveying of the seafloor. Repetitive surveys can be made to establish recurrence intervals for scours of different size in a particular location or pipeline route (Lewis and Barrie 1981). This method has some limitations, particularly its cost. Surveys necessitate the substantial expense of trained personnel, sophisticated equipment and ship time. The field measurement gives the size of the scour at the time of the survey. Sediments may be transported into the scour by bottom currents changing bottom relief. Also, there may be an infilling of the scoured trench in course of time due to the slumping of the sides. Annual variation in iceberg population density is

high (Fig. 3); this probably indicates similar high variation in annual scour formation. Therefore several years of observations are required to confidently establish recurrence intervals for scour activity.

Another approach to quantify the scour problem with respect to maximum scour dimensions, is to model the scour process mathematically and physically. This will be discussed below.

## 2.5 Iceberg Scour Models

The modelling of any engineering problem requires an understanding of the physical process and the associated variables. The mechanism of iceberg scouring is one in which the energy of a moving iceberg is dissipated as it plows into a sloping seabed of some type. Using this concept Chari (1975) developed a mathematical model and verified the geotechnical aspect of it in the laboratory.

### 2.5.1 Chari's model

An early attempt to evaluate iceberg scouring from a mathematical perspective was that of Chari and Allen (1972). Extensions, refinements and validations of the original theory have been well documented since then in a number of publications. (Chari and Allen 1974, Chari 1975, Chari and Guha 1978, Chari and Muthukrishnaiah 1978, Chari

1979, Chari, 1980, Chari et al. 1980, Chari and Peters 1981).

The three broad categories of iceberg scouring based on seafloor conditions were discussed earlier, (Fig. 1). In case C of Fig. 1, the bottom sediments are assumed soft and yielding with the iceberg plowing horizontally. This is the worst case from considerations of the maximum scour depth.

The geotechnical data reviewed earlier indicates a wide variation in the type of the seabed on the Canadian eastern shelf. The mathematical model developed so far is for the extreme condition and for computing the maximum likely scour depth. The idealized theoretical concept of the model is shown in Fig. 7. The iceberg is treated as a rectangular prismatic block whose strength is greater than the soil it contacts. This implies soil failure and not ice failure. The iceberg is assumed hydrodynamically stable and has some initial drift velocity as it travels perpendicular to the inclination of the slope. As the scour lengthens the iceberg progressively cuts deeper into the slope pushing soil ahead and to the sides in a manner similar to soil displacement around a bulldozer blade. The scour profile in the wake of the iceberg model consists of a depressed central trough with raised berms or shoulders on both sides. The resistance to iceberg movement is primarily the frontal passive resistance on the scouring face. The iceberg scoops

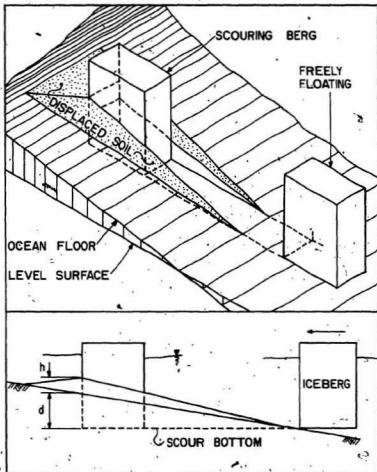


FIG. 7 IDEALIZED THEORETICAL CONCEPT OF ICEBERG SCOUR MODEL (CHARI 1979)

out a series of soil wedges and eventually stops when the available energy from the driving forces equals the energy used in displacing the soil. At any instant the frontal resistance to the iceberg is (Chari 1979):

$$P = \frac{\gamma'(h+d)^2}{2} B + \frac{2\tau dB}{\sin 2\theta} + \frac{\tau d^2}{\sqrt{2}} (1 + \cot \theta) \quad [1]$$

where:

P = soil resistance on front face of idealized iceberg.

$\gamma'$  = submerged unit weight of soil.

h = height of soil surcharge at any instant during scouring.

d = depth of scour at any instant during scouring.

B = width of idealized iceberg.

$\tau$  = shear strength (undrained) of soil.

$\theta = (\pi/4) - (\phi/2)$

$\phi$  = angle of soil shear resistance.

Assuming a cohesive soil, and under undrained conditions, the equation for iceberg scour has been given as:

$$\frac{WV^2}{2g} + C_d \rho \frac{ALV^2}{6} = \frac{\gamma'(H+D)^2 BL}{6} + \tau DLB + \frac{\sqrt{2}}{3} \tau D^2 L \quad [2]$$

where:

W = weight of iceberg.

V = initial velocity of iceberg.

g = acceleration due to gravity.

$C_d$  = drag coefficient.

$\rho$  = density of seawater.

A = projected area of submerged iceberg normal to propelling current.

L = maximum length of scour.

H = final height of soil surcharge.

D = maximum depth of scour.

The left hand side of [2] represents the energy available to drive the iceberg. This is dependent on the mass and velocity of the iceberg and also the current drag on the submerged portion of the berg. The right hand side of [2] represents the seabed resistance. It is dependent on the length, depth and width of scour, the surcharge dimensions, the effective unit weight and shear strength of the soil.

Laboratory verification of [2] is not possible in its exact form due to the constraints in scaling soil strength and grain size. Instead, experiments were designed to evaluate [1], the soil-iceberg interactive force. A tiltable glass sided tank 3.5 m long, 0.75 m wide and 0.7 m deep was fabricated and fitted with a towing carriage to support 230 mm wide iceberg models. A soft compressible clay was used for the sloped sediment bed. The total force on the model and the soil pressures on the different faces were continuously recorded as the model was pushed at constant velocity into the slope (Chari 1975). Good agreement was observed between theoretical and measured values of soil resistance. The iceberg scour model was thus found

satisfactory with respect to the mechanics of soil-iceberg interaction.

Eqn. [2] was used to predict the scour size for different combinations of field conditions. Table 5, Chari (1979), is the result of one such computation for a 200 GN (20 million ton) iceberg. Similar results have been published in the form of curves to show the influence of the individual variables on scour depth (Chari and Peters 1981). In general, equation [2] yields scour dimensions in the same range as those observed on the seabed. However, the scarcity of good input data such as iceberg size, shape, velocity, and seabed properties limits closer comparison and correlation between the predicted scours and actual measurements.

#### 2.5.2 Fenco's model

The Arctic Petroleum Operators Association (APOA) commissioned a report (APOA 69-1) on ice scours and the work was completed by Foundation Engineering Company of Canada (FENCO) in 1975 and subsequently published in Kivissild et al. (1981) and Kivissild (1981, 1982).

Two models were developed for predicting iceberg scour depth; a dynamic model and a minimization model. A third model presented in the report is basically the energy approach of Chari and Allen (1972) published earlier.

TABLE 5 PREDICTED ICEBERG SCOUR SIZE

W = 200 GM, B = 30 m, V = 0.5 m/sec

 $\gamma_{\text{sat}} = 15 \text{ kN/m}^3$ 

Seabed slope	$C_d$	$\tau$ (kPa)	Scour depth (m)	Scour Length (km)
1:100	0.1	2.5	9.7	0.97
	0.1	50.0	4.3	0.43
	0.5	2.5	15.0	1.50
	0.5	50.0	6.1	0.61
1:1000	0.1	2.5	6.7	6.70
	0.1	50.0	1.8	1.80
	0.5	2.5	14.5	14.50
	0.5	50.0	4.5	4.5

(Chari 1979)

The dynamic model assumes that the iceberg is a rectangular prismatic block having three degrees of freedom; heave, surge and pitch. Driving forces considered are due to wind, wave, current and pack ice. The soil resistance forces considered are the passive pressure on the front face and the soil reaction on the base of the iceberg. For the expected range of ice velocity of 2 knots (1 m/sec), soil displacements were treated as quasi-static and standard methods of soil analysis were used. The trial wedge method was used to evaluate the passive resistance on the front face of the iceberg treating the soil as a  $c-\phi$  material. For soil reaction on the base, three different approaches were used: a spring mass approach treating the soil as an elastic medium, the plastic equilibrium theory and an elastoplastic modification method. Results of the application of the dynamic model are shown in Table 6. The iceberg model considered was 21 m wide x 122 m long x 30.5 m deep. The ice block was also given an additional driving force in the form of a gradually increasing ice pack force. Calculated scour depths indicate that assumption regarding soil reaction on the base of the iceberg had little influence on the results.

The minimization model of FENCO assumes the ice block is always in static equilibrium during scouring. The iceberg scour is assumed to proceed as a continuous process in the dynamic model, while in the minimization method the

TABLE 6 ICEBERG SCOUR SIZE COMPUTED FROM FENCO MODEL

ICE BLOCK SIZE: .21 m WIDE x  
122 m LONG x 30.5 m DEEP

		Cohesive Soil Silty Clay	Granular Soil Sand
Cohesion	c	4.7 kPa	0
Internal friction angle	$\phi$	1°	20°
Ice - soil friction angle	$\delta$	0.5°	10°
Modulus of Elasticity	E	1358 kPa	0 on surface
Poisson's ratio	$\nu$	0.45	0.130
Subgrade modulus	k	39 kN/m <sup>3</sup>	spring constant K = 12 kN/m <sup>2</sup>
Effective unit weight	$\gamma$	5.9 kN/m <sup>3</sup>	5.9 kN/m <sup>3</sup>
Seabed slope	$\beta$	1°	1°
Drift speed	V	0.9 m/sec	0.9 m/sec
Gradually increasing ice pack force to 730 kN/m:			
Scour depth, D, assuming elastic soil reaction below ice		6.1 m	4.6 m
Scour length, L		320 m	240 m
Upward displacement		0.6 m	0.3 m
D assuming elastoplastic soil reaction below ice			4.6 m
L			240 m
Upward displacement			0.3 m
D assuming plastic soil reaction below ice		6.4 m	
L		293 m	
Upward displacement		1.2 m	
(Kivisild 1982)			

berg is assumed to move in individual thrusts. The iceberg moves horizontally similar to the energy model. Kivisild (1981) suggests the minimization solution is inapplicable in soft soils. Further the method gives a scour sizes smaller than that from the energy model.

The energy model given by FENCO in APOA 1975 is similar to that of Charf and Allen (1972), except that additional driving forces of pack ice and wind on the iceberg were considered in addition to the kinetic energy.

No experimental verification of FENCO's dynamic model appears to have been attempted, although suggestions such as towing an instrumented barge into a prepared sand slope are contained in the APOA report.

In summary the basic principle of mathematical modelling consists of equating the iceberg driving forces to the soil resistance. These models represent the extreme condition of scouring and attempt to compute the safe burial depths for the seabed installations.

### 2.5.3) Other models

There have been efforts by others to study the scour process (Abdelnour et al. 1981) however the results are not yet available in the open literature.

## CHAPTER III

## OBJECTIVES OF THE EXPERIMENTS

The primary objective of laboratory modelling of iceberg scours is to establish the validity of those aspects of the mathematical model which deal with the soil resistance to iceberg plowing. Chari (1975) conducted model tests in soft, cohesive soils using a 229 mm wide plexiglass instrumented model in a glass sided testing flume. These tests showed a difference between the computed and measured forces on the iceberg model (Fig. 8) and this difference was attributed to the deformations in the soil mass far ahead of the scouring iceberg. A zone of soil disturbance was observed well below and ahead of the laboratory model. Some preliminary measurement of the pressures was also reported (Chari 1975). One of the implications of this observation is that the theoretical estimates of scour sizes would be conservative. A phenomenon similar to that observed in the iceberg scour tests was also reported by Krause (1975) in reference to earth moving equipment in loose sands. It was therefore decided to continue the physical modelling of iceberg scours with models of various sizes and in cohesionless soils. It was also felt necessary to quantify the zone of soil disturbance ahead of the plowing model.

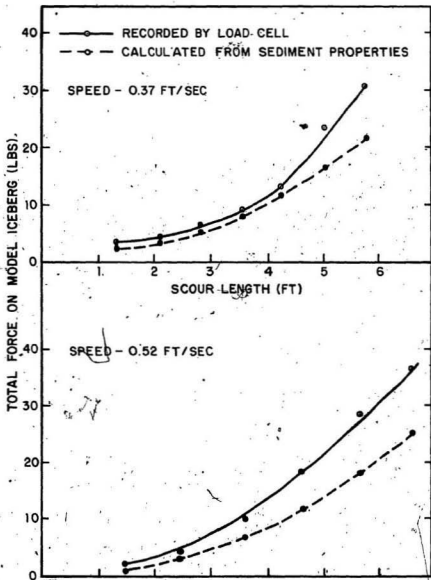


FIG. 8 COMPUTED AND MEASURED TOTAL PULL ON THE IDEALIZED BERG MODEL (CHARI 1975)

It was thus decided to embed an instrumented model pipeline inside the soil and to measure the pressures on the pipeline due to iceberg scour.

The scope of the experimental work and the different parameters used are as follows:

1. Soil type - cohesionless sand (detailed properties given later).
2. Iceberg model size - 230 mm wide models of earlier tests and new 500 mm wide models to investigate the scale effects.
3. Iceberg model shape - different keel shapes to investigate their effect on soil resistance.
4. Zone of influence - measure the pressures on an instrumented pipeline model to delineate the zone of soil movement.

The details of the equipment and experimental methods used are discussed in the following chapter.

## CHAPTER IV

## EQUIPMENT AND EXPERIMENTAL PROCEDURES

## 4.1 Description of Apparatus

The requirements of the equipment for this research were similar to those of Chari (1975) with the exceptions that the soil type is different and the iceberg model is larger. A towing tank with a variable speed carriage, instrumented iceberg models, pipeline models, and a soil test bed of reproducible properties were the other requirements. A detailed description of these components is given below.

## 4.1.1 Towing tank

A reinforced concrete tank approximately 14 m long x 6 m wide equipped with a tow carriage was used for these tests. A plan view and cross-section of the facility are shown in Fig. 9. The watertight tank had a centered dividing wall separating it into two rectangular flumes each 3 m wide x 0.83 m deep. The top of each of the longitudinal walls supported a guide track and chain-drive to carry a moving gantry or carriage. The gantry frame was made out of two 200 mm x 300 mm hollow rectangular steel beams spanning the 6 m tank width. One end of the steel beam was removable

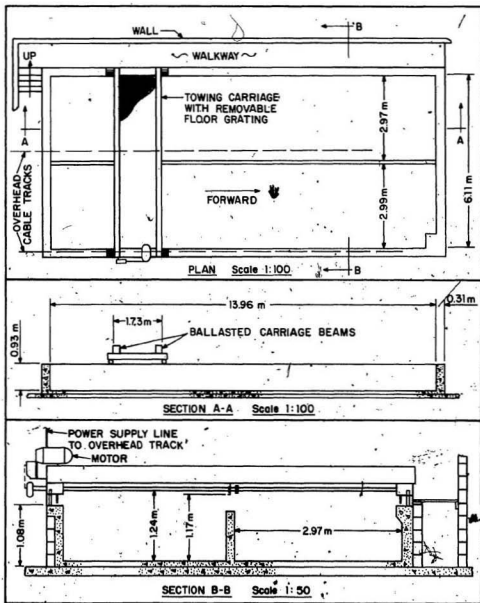


FIG. 9 PLAN AND CROSS-SECTION OF THE TOWING TANK

to provide combined storage for up to 1400 kg of counterweight in the form of 6 m lengths of steel reinforcing bar. The ballast was required to resist an overturning moment on the carriage when towing loads were high. The rectangular beams also provided an anchoring base for mounting the iceberg models and a soil rake system which will be discussed later. A removable floor of sectional open grating positioned between the beams provided a work area and supported the data acquisition equipment.

The carriage was powered by a 7.5 HP U.S. variable speed electric motor capable of constant towing speeds of 6 to 30 cm/sec. A calibration curve of carriage velocity and motor setting is given in Fig. 10. There was no measurable difference in carriage speed over the range of towing loads used in this research i.e. a motor setting of 1.0 corresponded to a carriage velocity of 9.5 cm/sec regardless of the type of iceberg model towed. Power was transmitted from the motor through a torque converter to a 62 mm diameter x 6.8 m long driveshaft. A sprocket on each end of the driveshaft engaged a chain track and pulled the carriage along the tank length. Carriage alignment perpendicular to the direction of travel was maintained by two V-groove 254 mm diameter wheels on the motor side of the tank and by properly maintaining tension in the chains. Periodic adjustment of the alignment was necessary to

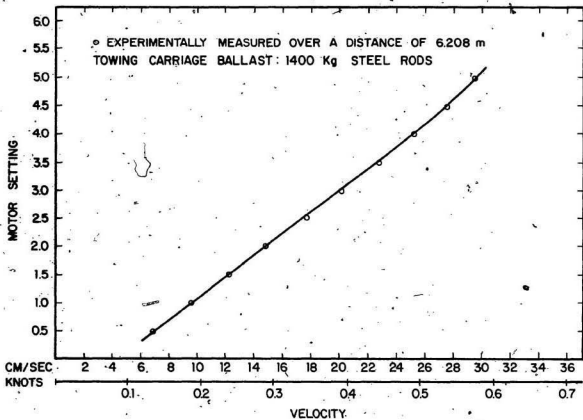


FIG. 10 CALIBRATION CURVE FOR THE TOWING CARRIAGE

minimize mechanical wear on the system. Operation of the carriage was from a fixed reversible switch near the motor or a portable watertight switch on a 5.m long cable. Carriage position along the tank was continuously measured during experiments by way of a potentiometer wire stretched along one side, which is described later in detail in section 4.1.5.

#### 4.1.2 Soil properties

A cohesionless dry sand was used as the representative seabed for the experiments. The properties of the soil are given in Table 7. This particular type of soil was selected for a number of reasons. The available geotechnical data for the continental shelf summarized in Chapter II, indicated a wide range of surficial sediment type from clays to sands and gravels. The experimental work of Chari (1975) used a soft compressible clay. To broaden that work it was decided to use another soil unlike clay and yet similar to the sediments on the shelf. About 18 m<sup>3</sup> of locally available masonry sand was selected. The maximum particle size was limited to 4.00 mm to provide compatibility with the existing soil pressure transducers whose sensing face was about 11 mm diameter. A grain size distribution curve for the sand is given in Fig. 11.

TABLE 7 PROPERTIES OF SOIL USED IN THE LABORATORY TESTS

Visual description		light brown cohesionless sand
Uniformity coefficient	$C_u$	6.3
Max. grain size		4.76 mm
Grain shape		angular to subangular
Max. dry density	$\gamma_{max}$	19.7 kN/m <sup>3</sup>
Min. dry density	$\gamma_{min}$	15.7 kN/m <sup>3</sup>
Experimental dry density	$\gamma_{exp}$	17.1 kN/m <sup>3</sup>
Water content	w	Approx. 0.3% (air dried)
Angle of internal friction at $\gamma_{exp}$ (from direct shear and triaxial tests)	$\phi$	35.5°
Soil type		SW-SM

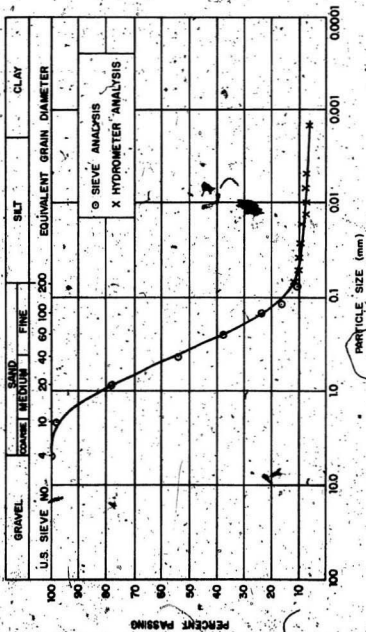


FIG. 11 GRAIN SIZE DISTRIBUTION CURVE FOR THE SOIL USED IN THE TESTS

#### 4.1.3 Iceberg models

A total of six different iceberg models were used for this research. The relevant features of each are summarized in Fig. 12. Two model widths of 500 mm and 229 mm were used. The maximum model width was limited by the 3 m inside dimension of the flume. The tank allowed a net usable soil test bed width of 2.5 m after a strip 0.25 m wide on both sides was provided to make the tank accessible during the sample preparations. This left a 1 m undisturbed soil test bed on both sides of the 500 mm iceberg model to eliminate any side effects of the tank wall on the tests. Towing tests with models wider than about 500 mm would probably have required removal of the center dividing wall.

All models were constructed of 6 mm thick 5052H32 grade aluminum sheet, except the flat plate models, L3 and S3 which were of 12 mm aluminum sheet for additional stiffness. External corners and edges were rounded to a radius of 6 to 7 mm. The corrosion resistant aluminum had additional advantages of strength and lightness. All the iceberg models were made very rigid compared to the soil. Strains and deflections of the models were negligible compared to the soil deformation. This accounts for the worst scenario to be expected in the field in terms of maximum soil disturbance and scour depth, when the iceberg is very stiff compared to

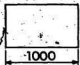
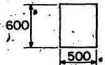
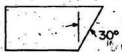
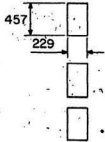
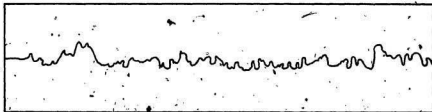
DESIGNATION	DESCRIPTION	PROFILE (mm)	FRONT VIEW (mm)
L1	RECTANGULAR BLOCK		
L2	RECTANGULAR BLOCK WITH 30° INCLINED FRONT FACE		
L3	FLAT PLATE		
S1	RECTANGULAR BLOCK		
S2	RECTANGULAR BLOCK WITH 30° INCLINED FRONT FACE		
S3	FLAT PLATE		

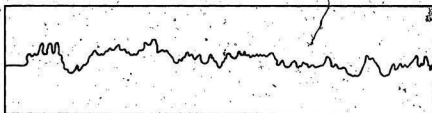
FIG. 12 SIZES, SHAPES AND IDENTIFIERS OF THE ICEBERG MODELS USED IN THE EXPERIMENTS

the seabed. Faces of the iceberg models had threaded holes to allow flush mounting of soil pressure transducers.

In order to determine the model-soil surface friction, the surface roughness of the aluminum sheet was quantitatively determined. Representative samples were cut from a similar sheet of aluminum and surface roughness tests were carried out using a Rank Taylor Hobson 'Talysurf 4' surface roughness instrument. Surface undulations had a maximum height of 0.0051 mm and a maximum wavelength of 0.64 mm. The results of two typical tests of surface roughness are shown in Fig. 13. A series of experiments were also performed to determine the skin friction  $\delta$  between the sand and aluminum. The tests were performed in a conventional 60 mm shear box at a constant rate of displacement in which the bottom part of the box was fitted with a block of solid aluminum of surface roughness similar to the iceberg models. The top part of the shear box was filled with sand at the same density as used in the scour tests. Normal stress levels of 56 to 187 kPa were used and tangential or horizontal stresses were measured over a time period of 5 to 8 min. (Fig. 14). In all the tests the horizontal stress tended to reach a maximum value and level off. A graph was drawn of maximum tangential stress and normal stress (Fig. 15). The friction angle  $\delta$  was measured to be 23°.



TEST # 1



TEST # 2

SCALE

HORIZONTAL 20:1

VERTICAL 2000:1

FIG. 13. SURFACE ROUGHNESS OF THE ALUMINUM USED FOR THE ICEBERG MODELS

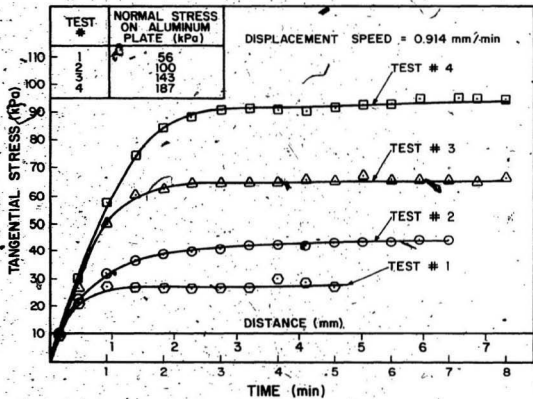


FIG. 14 SOIL-ALUMINUM FRICTION (60 mm SHEAR BOX TESTS)

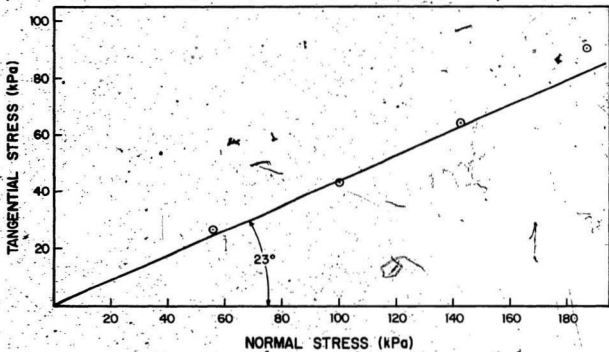


FIG. 15 SHEAR ENVELOPE: SOIL-ALUMINUM SKIN FRICTION TESTS

Two mounting frames were built to rigidly fix the various models to the towing carriage. Models L1 and L2 were supported on an aluminum frame constructed of 100 mm x 100 mm hollow square cross section beams. Details of the frame and the method of securing L1 and L2 are shown in Fig. 16. Both models were fixed to the frame by a horizontal swing plate arrangement at the front and back. During scouring, horizontal movement parallel to the direction of travel was resisted only by two compression load cells operating in tandem. The total horizontal force required to penetrate the soil slope was the sum of the two load cell measurements. Horizontal forces perpendicular to the direction of scour were not directly measured, nor were vertical forces. However, pressure transducers were used to measure soil resistance on the front, sides, and bottom of the iceberg models. This is further discussed in a later section.

A separate frame was necessary to use the narrower 229 mm models and the flat plate models. The iceberg models, S1, S2, S3 and L3, were used on a mounting frame constructed of 50 mm x 50 mm steel angle and 100 mm steel channel (Fig. 17). The models were rigidly fixed during the experiment. Provision was made to measure soil pressures on S1 and S2 and horizontal forces on L3 and S3.

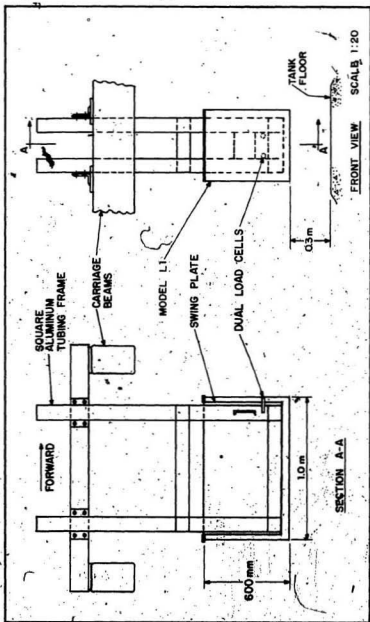


FIG. 16 MOUNTING FRAME FOR ICEBERG MODELS L1 AND L2

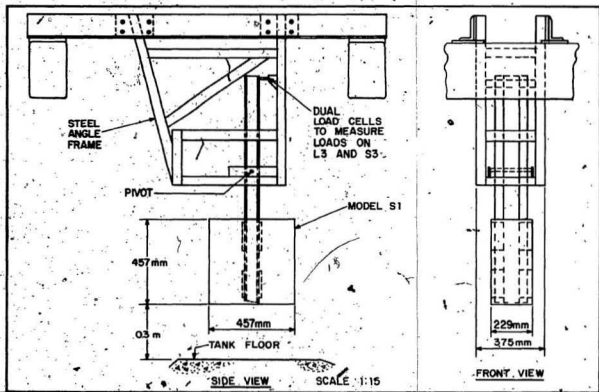


FIG. 17 MOUNTING FRAME FOR ICEBERG MODELS S1, S2, S3 and L3

Both iceberg model mounting frames can be centered in the soil test bed by bolted connections to heavy steel angles anchored to the main beams of the towing carriage. Clearance between the bottom of the iceberg model and the tank floor can be adjusted from 300 mm to 500 mm depending on experimental requirements.

#### 4.1.4 Pipeline model

The model pipeline is shown in Fig. 18 and Fig. 19. The pipe, of octagonal cross section, with a maximum diameter of 132 mm and 0.76 m long was constructed of 12 mm plexiglass sheet. It was assembled in longitudinal sections whose mitered joints were bonded with chloroform. The pipe was designed to be very rigid in comparison to the soil as this would be the condition for the development of maximum soil pressure on its external wall. Threaded holes in the pipe wall accommodated flush mounted pressure transducers identical to those in the iceberg models.

One end of the pipeline was removable to permit installation of the transducers and cables. A 38 mm diameter x 6 m long flexible hose (Goodyear Plycord) on the same end of the pipe was used to house the signal cables and protect them from damage. The pipeline model was held by plywood templates at both ends which were in turn bolted to an aluminum frame anchored to the tank floor. The depth of pipe

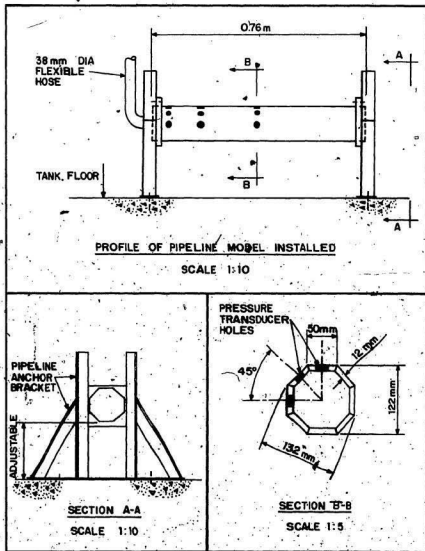


FIG. 18. DETAILS OF THE PIPELINE MODEL

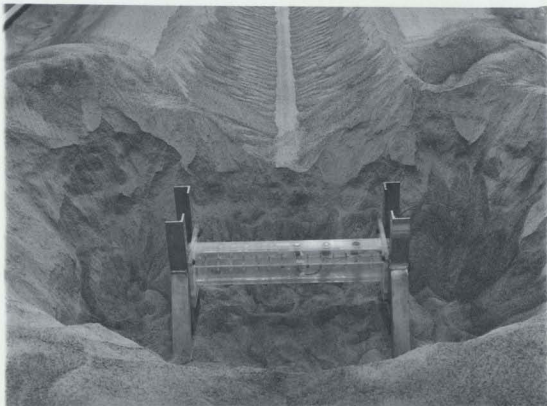


FIG. 19 PHOTOGRAPH OF THE PIPELINE MODEL AFTER AN EXPERIMENT

burial as well as its position relative to the scour were adjustable. For this study the pipeline was oriented perpendicular to the direction of scour and aligned so that the pipe was in the middle of the scour track.

#### 4.1.5 Instrumentation

The primary requirement of the instrumentation system was to continuously monitor and record soil pressures and soil resistance on the iceberg and pipeline models during each experiment. Each experiment required 90 to 120 seconds from start to finish with data being recorded continuously. A flowchart of the data acquisition system is shown in Fig. 20, and a description is given below.

As scour experiments required an 8 to 11 m travel of the tow carriage a method of accurately recording carriage position along the tank was necessary. This was achieved by stretching a potentiometer wire along the walkway side of the tank. A D.C. power supply unit on the carriage applied a constant 3.00 volts to the potentiometer wire through cables soldered at each end. The voltage supply line was routed overhead on one of two cable roller track assemblies indicated in Fig. 9. A copper contact fixed to the carriage slid along the potentiometer wire as the carriage moved. The linearly changing voltage between the beginning of the wire and the carriage contact was recorded

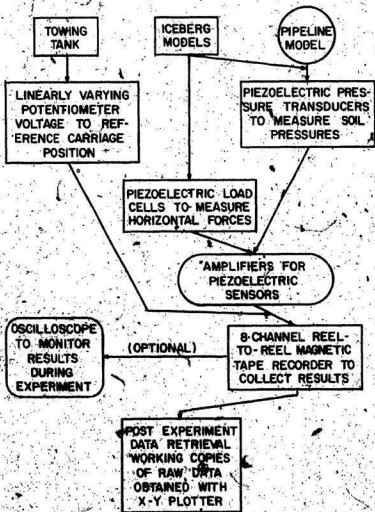


FIG. 20 FLOWCHART OF THE INSTRUMENTATION USED FOR THE ICEBERG SCOUR EXPERIMENTS.

for each experiment. The position of the contact on the carriage could be varied to align with the front edge of the iceberg model. A permanent reference scale with 0.001 m graduations was attached parallel to the wire to check calibration.

The sensors used in the experiments to measure loads and soil pressures were piezoelectric type quartz transducers manufactured by Kistler Instrument Company. Specifications and calibration procedures for the load and pressure sensors including the tests for cross face sensitivity for the pressure transducers are detailed in Appendix A. Each unit had a quartz element housed in a hermetically sealed stainless steel shell. Mechanical forces or pressures applied to the quartz crystal caused a potential difference across the crystal proportional to the applied stress. Each sensor was used with an amplifier on which was set the individual sensitivity number for that sensor as supplied by the manufacturer. The D.C. voltage output from each amplifier was recorded on the 8 channel recorder. Typical amplifier outputs were 68.95 kPa/volt for the pressure transducers and 2.23 kN/volt for the load cells.

For the experiments, the amplifiers, tape recorder, x-y plotter, multimeter, voltage calibrator, oscilloscope and power supply were set on custom built work benches resting on the grating floor of the tow carriage to

minimize cable lengths. When pipeline experiments were in progress the amplifiers required for the pipeline transducers were positioned near the pipe to reduce signal cable length. This increased the output cable length from the amplifier to the recorder by 4 to 5 m but did not affect the signal.

An oscilloscope was frequently used to monitor results as they were being recorded by the tape recorder. This was useful during the pipeline tests as it provided a visual display of soil pressure on the pipe when the iceberg model scoured near the pipe. Following the experiment, the recorded results were played back on a x-y plotter with the potentiometer wire voltage providing the horizontal reference axis. Typical experimental results are presented in Chapter V of this thesis.

#### 4.2 Preparation of the Soil Test Bed

A method was to be devised to control the properties of the 18 m<sup>3</sup> of sand to ensure repeatability of the soil properties. The soil was 0.2 m deep at the shallow end and 0.6 m deep at the other end when placed in the 14 m x 3 m tank at a slope of 1:35. One method of sample preparation is to remove the soil prior to each test and replace it by a controlled raining technique. This approach has been successfully used for placing dry cohesionless material of quantities less than 1 m<sup>3</sup> for other laboratory

applications. Due to the large volume of sand for the iceberg tests the raking method was not found to be practical. Another method of controlling sand properties for laboratory tests is that used by Wilson and Franklin (1971). In a rectangular tank whose cross sectional area was just less than  $1 \text{ m}^2$ , sand was placed on top of a porous sheet through which was forced sufficient air to fluidize the soil thereby changing effective density. This method precluded the necessity of taking the soil out of the tank. However, the cross-sectional area of the test bed for iceberg research which was  $42 \text{ m}^2$ , was too large for fluidization.

Based on experimentation with a number of soil rakes attached to the towing carriage, a raking system which produced very consistent sand densities was designed. The four pronged rake and its support frame are shown in Fig. 21. The position of the rake along the tank width was adjusted by sliding the rake support along a rigid T-shaped track on the forward carriage beam. A series of vertically spaced studs on the rake facilitated the process of raking down to various predetermined heights off the tank floor.

A standardized raking pattern was established by making a set number of passes at a depth for constant towing speeds of 95 mm/sec. The procedure was to position the carriage as close as possible to the shallow end of the tank. A trench was excavated down to the tank floor along the width

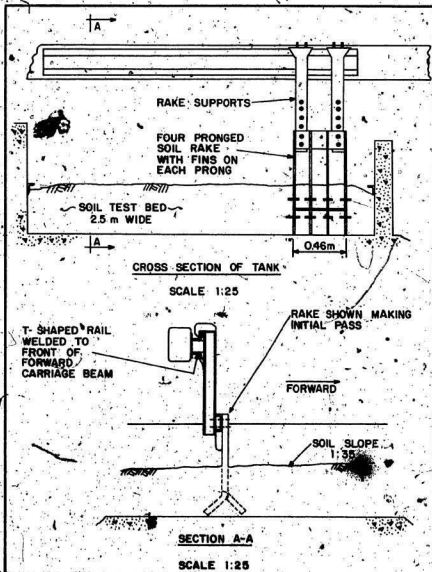


FIG. 21 THE RAKE SYSTEM FOR SOIL TEST BED PREPARATION

of the tank. The 0.46 m wide rake was bolted on in its lowest position (approximately 10 to 15 mm from the floor) on one side of the tank leaving an unraked strip 0.25 m wide along the edge of the soil test bed. The carriage was moved up and down the tank raking a section 0.46 m wide x 10 to 11 m long. Then the rake was kept at the same cut depth but moved 75 mm toward the other side of the tank and the process repeated. This allowed for a mixing of the soil between the 150 mm spaced rake tynes of the first pass. The rake was then moved laterally another 0.5 m towards the far side and another 0.46 m swath was raked. The process was continued until raking reached the opposite side of the tank. The entire process took 45 to 75 minutes. Following raking, the soil was smoothed out by hand using customized garden rakes. The final grade of 1:35 was achieved by drawing a cedar board up and down the slope trimming off the excess and filling in minor depressions as required. Each end of the board was supported by an aluminum template (Fig. 21) anchored to the two sides of the inside of the tank wall along its 14 m length.

#### 4.3 Experimental Procedure

In order to allow comparisons between individual scour experiments, a standard procedure was adopted for conducting each test. Preparation for a test commenced

with raking and grading the soil test bed as detailed in the previous section. The iceberg model to be used was then bolted in position. The instrumentation system was set up and checked for correct operation. Preliminary measurements of carriage position and initial instrumentation settings were noted. All instrumentation was turned on at least 20 minutes prior to the test as recommended by the operating manuals for the various instruments.

The scour test was started by simultaneously activating the tow carriage and the recording system. The duration of each scour experiment was 90 to 120 sec. with 3 to 4 hrs generally required for the preparation prior to the test. A photograph of an experiment in progress is shown in Fig. 22. The iceberg model shown in Fig. 22 is the 500 mm wide rectangular L1. Another view of the same iceberg model L1 is shown in Fig. 23. This shows the scour profile formed in the soil test bed at the end of the scour test. The iceberg model was stopped and the test terminated when the leading face of the model was about 2.0 to 2.5 m away from the end wall of the tank giving a maximum scour length,  $L$ , of just over 8 m and a maximum scour depth,  $D$  of about 0.23 m. At the end of the test the final position of the carriage was recorded and the instruments turned off.

Depending on particular experiment requirements, measurements of soil density and penetration resistance were



FIG. 22 AN EXPERIMENT IN PROGRESS WITH ICEBERG MODEL L1

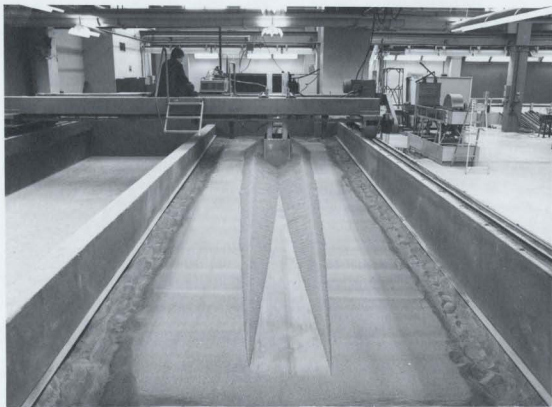
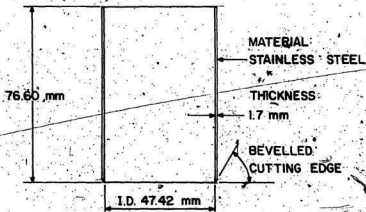


FIG. 23 SOIL TEST BED AFTER A SCOUR EXPERIMENT

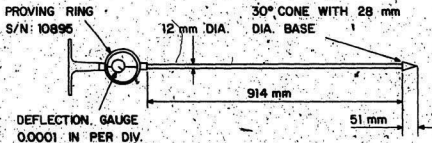
made inside and outside of the scour track using a thin-walled cylinder and a hand-held penetrometer (Fig. 24). Other methods of in situ density measurement such as the sand cone and rubber balloon techniques were attempted but found unsuitable in the dry medium dense sand used for these experiments. Both these devices measure the volume of a known weight of soil excavated from a small area of the soil and are better suited to dense materials.

For each scour test it was useful to record all the pertinent data on standardized check list and data sheets designed to meet the requirements of the experiments. Appendix B is a typical set of data sheets for one experiment. This method was advantageous because it saved time during the tests and lessened the chances of overlooking data. The experimental results of soil pressure and load for the various tests were reproduced on standard size graph paper following the test and stored with the data sheets for that experiment for further analysis.

Besides the usual measurements of soil pressure and load on the iceberg models it was necessary to measure the dimensions of the soil surcharge piled up (Fig. 22) in front of the advancing model. The theoretical calculation of soil resistance at any point along the scour length, given by equation [1], requires the height and length of the soil surcharge. Two experimental methods were used to obtain



CROSS-SECTION OF THIN WALL DENSITY SOIL SAMPLER  
SCALE 1:125



HAND OPERATED STATIC CONE PENETROMETER  
SCALE 1:10

FIG. 24 DETAILS OF THE EQUIPMENT FOR MEASURING IN SITU  
PROPERTIES OF THE SOIL TEST BED

these values. Initially, individual experiments were conducted in which the soil test bed was prepared in the usual manner as described earlier in section 4.3. The iceberg model was advanced about 0.5 m, stopped and the surcharge height, and length, and the exact scour length were physically measured. The model was advanced another 0.5 m increment and the process repeated for the whole scour length thereby producing a relatively continuous record of the surcharge dimensions. To investigate the errors associated with stopping and starting the iceberg model, a Haselblad camera with automatic rewind and flash was fixed to the towing carriage. The camera was positioned to photograph a profile of the surcharge and a scale which was previously attached to the front of the iceberg model. The scour test was run continuously, as for a regular experiment, with a photograph being obtained every 4 seconds (approximately every 0.4 m of scour length). The flash of the camera was also a cue to mark the voltage on the potentiometer wire, which then provided a reference scour length for each photograph. Following the test, each exposure was reproduced on 75 mm x 125 mm print paper for analysis. Surcharge dimensions were measured directly off the photographs by using the reference scale. Repeated comparisons of surcharge dimensions, obtained by direct measurement and from photographs showed no appreciable variation due to the method.

used.

The results of the experiments along with an interpretation and analysis of the data are presented in the following chapter.

## CHAPTER V

## EXPERIMENTAL RESULTS AND DISCUSSION

## 5.1 General

The experimental program was divided into two main areas:

- 1) Measurement of soil forces and soil pressures on various shapes and sizes of iceberg models, to understand the type of iceberg-seabed interaction.
- 2) Measurement of soil pressures on the model pipeline, embedded at different locations relative to the iceberg scours in order to delineate the zone of soil movement in the vicinity of a scouring iceberg.

Other related experiments were also conducted to further examine the interaction between the scouring iceberg model and the soil. These included qualitative tests to examine the soil failure pattern associated with the scour process, quantitative tests to measure the soil displacements during scouring and quantitative tests to study the scour profile formed by the laboratory iceberg model.

Summaries of some of the results of this research were presented earlier (Chari and Green 1981, Green and Chari 1981, Chari et al. 1982, Green et al. 1983). These results are further discussed in detail in this chapter.

## 5.2 Tests on Iceberg Models

### 5.2.1 Iceberg scour profile

Observations of actual iceberg scours on the seafloor have shown that the scour features generally consist of a long, straight or curvilinear trench flanked on either side by a ridge or berm of soil. As discussed in section 2.4 attempts have been made to utilize the measured physical properties of iceberg scours, such as length and depth, to predict scour frequency and maximum scour depth. However, such direct application of field scour data may have inherent problems as demonstrated in the laboratory and discussed below.

The scour formed in the laboratory (Fig. 23) was similar in general form to actual scours that have been identified on the sea bottom. The laboratory scour was characterized by a depressed central portion and raised embankments on both sides. Following a typical scour experiment, measurements of the scour profile were obtained at regular intervals along the scour length (Fig. 25). The figure shows three cross sections of the scour at the 2, 4 and 6 m scour length intervals. The heavy line indicates the actual scour profile formed during the experiment while the dashed line indicates the outline of the iceberg model during the process of scouring and hence this also identifies the

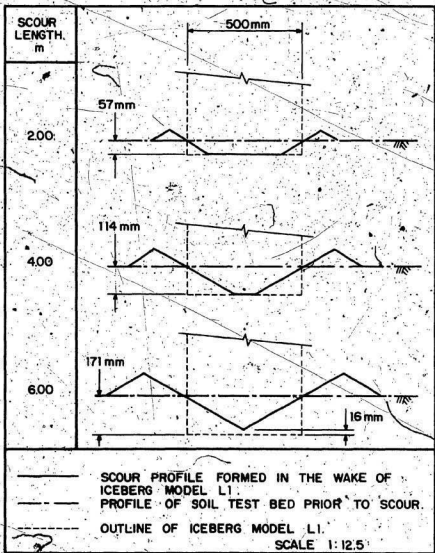


FIG. 25. PROFILE OF SCOUR CROSS-SECTION PERPENDICULAR TO THE SCOUR LENGTH

maximum scour depth. From the measurement of the scour profile at the 2 and 4 m location (Fig. 25) it is possible to identify the maximum depth of penetration of the iceberg model, however at the 6 m cross-section the scoured soil infills the trench and the actual scour is 10% deeper than the maximum depth of the V-shaped scour trench. A similar infilling process of the scoured trench is likely to happen on the ocean floor for a typical iceberg scour track. Thus the observed (and measured) field scour depth would be an underestimate of the original depth of maximum scour. The type and degree of infilling of the scour track, whether it is the laboratory model or an ocean bottom iceberg scour track, would be a function of the shape and width of the iceberg keel, the depth of the scour and the natural slope angle of the soil. Therefore field measurements and the interpretation of maximum scour depth thereof may not represent the actual scour depths.

Additional considerations related to sediment dynamics and wave induced pore water pressure inside the soil will influence the shape of the scour trenches in the ocean bottom. The degree of such influence will depend on the age of the scour. Further, if the scour is formed in an area of active sedimentation, the feature may become partially obscured in course of time. Masking or obliteration of scours due to sediment movement, if substantial, could have

significant influence on the form of the scour profile. For example, Lewis and Barrie (1981) conclude that in the Hibernia area of the Grand Bank (Fig. 4) extreme winter storms or intrusions of the Labrador Current are sufficient to move surficial sediments thereby changing the appearance of bedforms such as scours. Water depth in the area is approximately 80 m which would create a shallow water situation (water depth  $< 1/2$  wavelength) under storm wave conditions. The seafloor sediments, which consist of sands and gravel (Lewis and Barrie 1981), would thus be susceptible to movement under those conditions.

Any field data on iceberg scour dimensions must therefore be viewed in light of the fact that the original scour dimensions may have been altered. The degree of change of the scour dimensions requires knowledge of a number of variables as noted above that may be particular to each iceberg scour. Therefore, it may not be prudent to predict, or extrapolate extreme events for iceberg scour based solely on the evidence of observed features.

#### 5.2.2 Soil resistance on iceberg model L1

One of the objectives of the experiments was to validate the mathematical model discussed in Chapter II with respect to the soil resistance to scour. The scouring process was assumed to occur as shown in Fig. 7 and was

simulated in the laboratory. The soil test bed was prepared as described in Chapter IV. Experiments were conducted initially with the 500 mm wide rectangular iceberg model L1 (Fig. 12). The iceberg model was towed at a constant speed of 9.5 cm/sec into the 1:35 soil slope. The total horizontal load on the iceberg model as well as soil pressures on the front side and base of the model were measured. The results of soil pressure measurements are discussed later. A typical force record for iceberg model L1 is shown in Fig. 26. This figure shows the type of increase of the horizontal load as the model penetrated the soil slope. The force record is similar in form to the results obtained by Siemens (1963) and Chari (1975).

The saw tooth form of the load curve (Fig. 26) was repeatedly observed during tests with all the iceberg models. The ratcheting type action of the horizontal force record appears to be due to the successive build up and failure of shear surfaces within the soil directly in front of the iceberg model. Subsequent peaks on the force record are higher as the model scours deeper into the soil slope. Similar soil failure patterns due to a horizontally advancing body have been observed by others. Chari (1975) reported a similar mechanism during modelling of iceberg scouring in soft cohesive soils. Siemens (1963) used a glass sided tank and a granular soil and correlated the appearance of failure

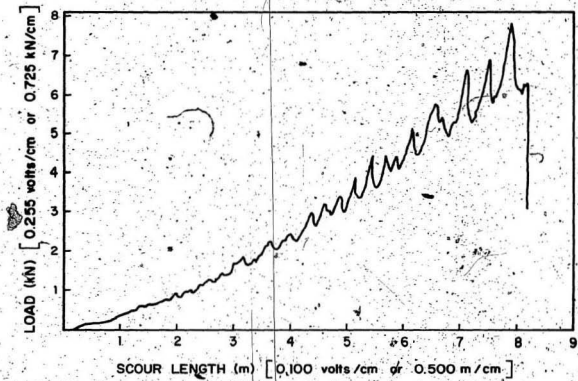


FIG. 26 TYPICAL HORIZONTAL FORCE RECORD FOR ICEBERG MODEL L1

surfaces in front of tillage equipment models (Fig. 27) with sudden decreases in load on the soil cutting blades.

The development of successive failure surfaces was also investigated qualitatively. The soil was prepared as described earlier. Iceberg model L1 was positioned approximately midway along the scour length with an initial scour depth of 143 mm. The soil slope was carefully graded to the 1:35 slope (Fig. 28-0). The model was advanced in stages by towing at a speed of approximately 6.5 cm/sec and photographs were taken at each stage (Fig. 28; 1-4). The stages in which the model was advanced was decided by the appearance of a failure wedge in front of the iceberg model as visually observed by a demarcated line in front of the iceberg. It may thus be seen that in Fig. 27-1 there is one clearly identifiable failure surface and in Fig. 27-2 to Fig. 27-4 the number of visually identifiable failure surfaces gradually increase. Conceptually, each failure surface may be identified with a peak in the force record of Fig. 26. The failure mechanism in front of an advancing iceberg model was also continuously recorded on video tape which illustrates the phenomenon graphically.

In conjunction with examining the general pattern of the load increase and the soil failure phenomenon discussed above, repetitive tests were conducted to measure the total horizontal load on the iceberg model L1. Based on

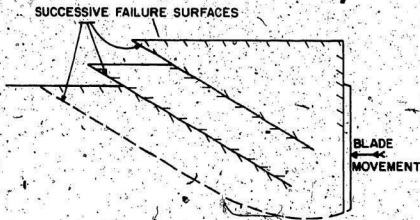


FIG. 27 SOIL FAILURE ALONG SUCCESSIVE SHEAR PLANES IN FRONT OF EARTHMOVING MACHINES. (SIEMENS 1963)

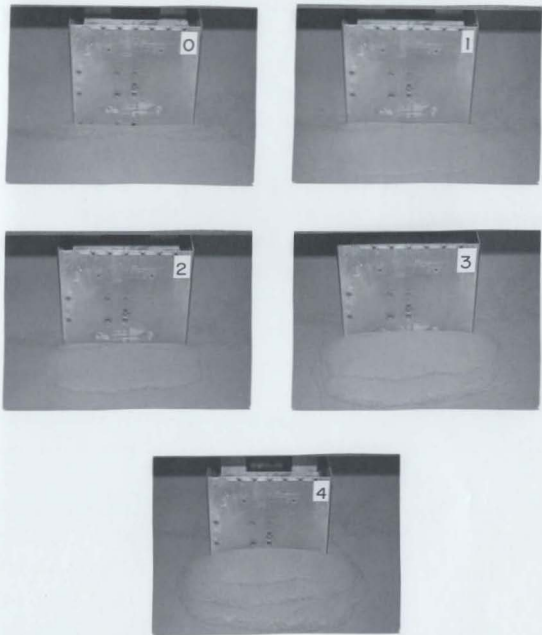


FIG. 28 SUCCESSIVE FAILURE PLANES IN FRONT OF ICEBERG MODEL L1

more than 20 repeated tests and from force records similar to that shown in Fig. 26 the maximum horizontal force of the iceberg model at different points along the scour track was obtained and the curve of maximum force is shown in Fig. 29.

Simultaneously with load measurement on iceberg model L1, soil pressures were continuously measured during the scour tests. Transducers were mounted on the front, side and base of iceberg model L1 (Fig. 30). The pressure transducers were spaced on the centerline of the front face as already discussed in Chapter IV. Typical results of the pressures on the front face of the model are also shown in the figure. The measured soil pressure was maximum near the toe of the model and decreased gradually towards the top. The variation of the soil pressure on the front face at different positions along the 8 m scour length is shown in Fig. 31. The general pattern of the measured pressures on the front face of the model is similar to that observed for tests in clay (Charl 1975). In those iceberg scour tests in soft cohesive soils it was shown that the soil resistance on the iceberg model was largely due to the passive soil pressures developed on the front of the model. A similar investigation was undertaken in this research for the case of a granular frictional soil.

If the measured pressures on the front face of iceberg model L1 (Fig. 31) are assumed constant over the

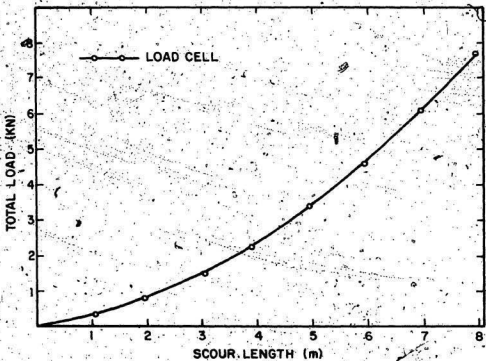


FIG. 29 TOTAL HORIZONTAL FORCE MEASURED ON ICEBERG MODEL L1

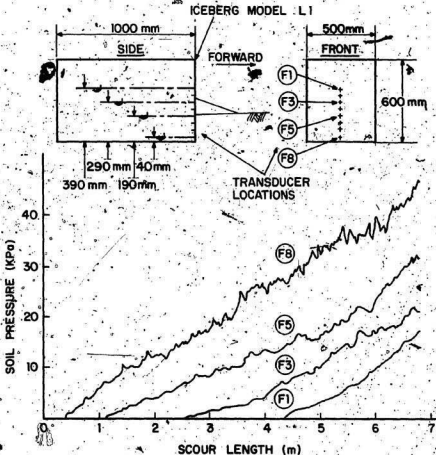


FIG. 30 TYPICAL RESULTS OF SOIL PRESSURE MEASURED ON THE FRONT FACE OF ICEBERG MODEL L1

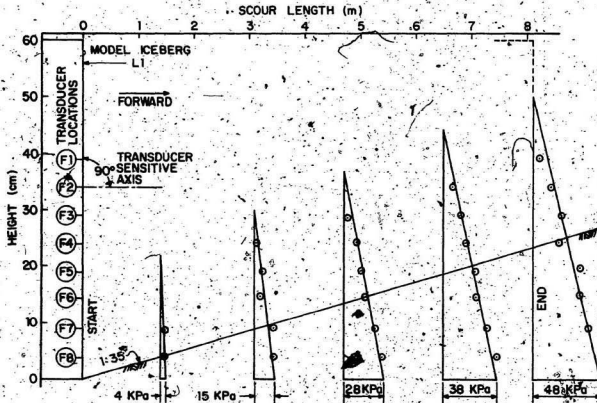


FIG. 31 VARIATION OF SOIL PRESSURE ON THE FRONT FACE OF MODEL L1

500 mm width, the load on the front face may be computed (Fig. 32). The load obtained from the pressure measurements on the front face is less than the total measured load. One of the reasons for this variation is that the load determined from the pressure measurements does not account for the frictional resistance of the soil on the sides and base of the model. In cohesive soils Chari (1975) showed friction effects to be negligible. For a cohesionless soil the influence of friction on the scour process was investigated as discussed below.

#### 5.2.3 Effect of Friction

Neglecting the frictional resistance of the soil, the iceberg scour equation [2] which was presented and discussed in Chapter II is:

$$\frac{WV^2}{2g} + C_d \rho \frac{ALV^2}{6} = \frac{\gamma(H+D)^2 BL}{6} + \tau DLB + \frac{\sqrt{2}}{3} \tau D^2 L \quad [2]$$

The solution of the equation for some assumed soil parameters and iceberg dimensions is shown in Fig. 33 (Chari and Green 1981). If it is assumed that the scouring iceberg is always neutrally buoyant and if the seabed material is a frictional soil, the soil pressure on the sides will cause additional resistance to the scouring process. Assuming the soil pressure on the sides as an active pressure the equation was modified as eqn. [3]. (Chari and Green 1981):

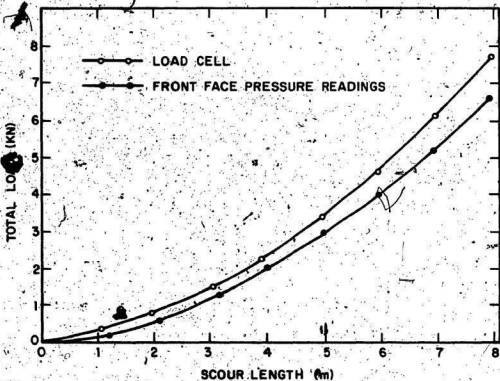


FIG. 32 COMPARISON OF THE TOTAL MEASURED LOAD ON ICEBERG MODEL L1 WITH THE 'LOAD ON THE FRONT FACE

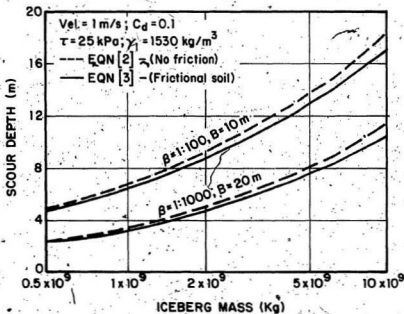


FIG. 33 INFLUENCE OF FRICTION ON THEORETICAL SCOUR DEPTHS (CHARI AND GREEN 1981)

$$\frac{wV^2}{2g} + C_D \rho \frac{ALV^2}{6} = \gamma' \frac{(H+D)^2 BL}{6} + \tau DLB + \frac{\sqrt{2}}{3} \tau D^2 L + 0.1 \gamma' BD^2 L \quad [3].$$

In the above equation, the  $\tau$  is the average shear strength along the surface of rupture and has to be evaluated in terms of the angle of shear resistance  $\phi$  and the overburden pressure. The solution of eqn. [3] is also given in Fig. 33 and it was shown that the difference in the theoretical estimation of scour depth would be in the order of 10% when the side friction is neglected. The above conclusions were experimentally verified and discussed below.

Soil pressures were measured on the side and base of iceberg model L1 and compared with the front face pressures (Figs. 34 through 36). The soil pressure on the sides was about 30% of that on the front face for corresponding heights above the base. The soil pressure measured on the base was about 35% of the maximum front face pressures. The maximum soil pressure on the front face, side and bottom were approximately 50, 18 and 20 kPa respectively.

Tests were conducted (Fig. 15) to determine the friction angle between the soil and the material of the iceberg model. This was found to be 23°. Three arbitrary points were selected along the scour length at 2, 5 and 8 m to determine the effect of friction. For each location the soil pressure distribution on the base and the sides was determined from the pressure transducer results as given in

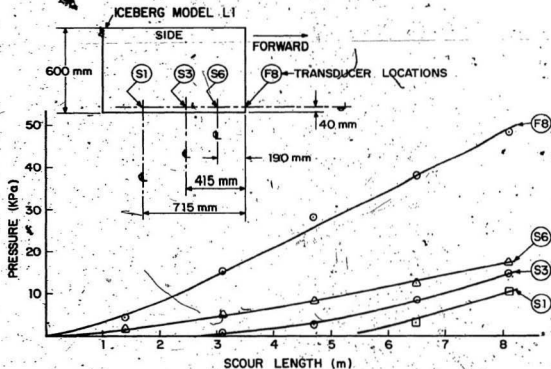


FIG. 34 COMPARISON OF SOIL PRESSURE ON THE FRONT AND SIDE OF MODEL L1, 40 mm ABOVE THE BASE

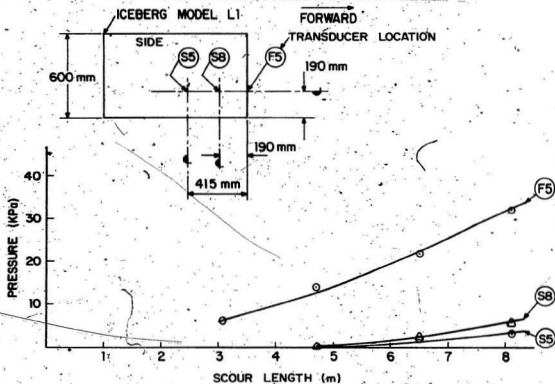


FIG. 35 COMPARISON OF SOIL PRESSURE ON THE FRONT AND SIDE OF MODEL L1, 190 mm ABOVE THE BASE

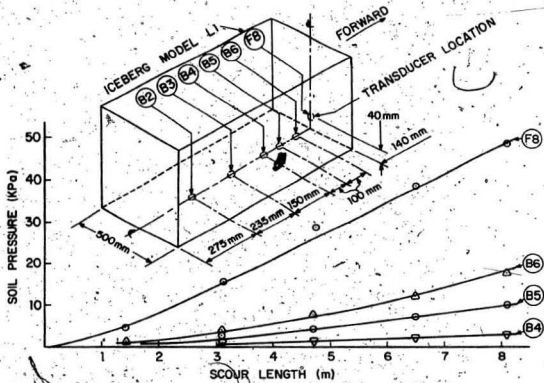


FIG. 36 COMPARISON OF SOIL PRESSURE ON THE FRONT AND BASE OF MODEL L1

Figs. 34 through 36. The contact area between the soil and the model was determined by direct measurement in separate experiments. From the measured normal pressures and the pressure distribution, and from a knowledge of the wall friction, the frictional forces on the base and the two sides were calculated and are tabulated in Table 8. The measured load on the model is compared with the individual components of the force on the front, sides and bottom in Table 8. The combined effect of the resistance on the base and sides is in the order of 10 to 14% of the measured total load on the iceberg model (Fig. 37). This is in conformity with the theoretical calculations. If the components of load on the front, base and sides, as determined from the pressure transducer measurements, are added the result will be as shown in Fig. 37. The total measured load is slightly greater than the sum of the loads calculated from the pressures. This is likely due to soil movement and compression in front and below the scouring iceberg model, and is discussed in a subsequent section.

#### 5.2.4 Theoretical computation of soil resistance

Theoretically the resistance to the front face of the iceberg model is given by eqn. [1] as follows:

$$P = \frac{\gamma(h+d)^2}{2} B + \frac{2\gamma dB}{\sin 2\theta} + \frac{\gamma d^2}{\sqrt{2}} (1 + \cot \theta) \quad [1]$$

TABLE 8 EFFECT OF FRICTION ON TOTAL LOAD FOR ICEBERG MODEL L1

	Scour Length (m)	Avg. Soil Press (kPa)	Contact Area (m <sup>2</sup> )	Equiv. Force (kN)	x tan 23° (kN)	Total Meas. Force (kN)	% of Total Meas. Force	
<u>Base</u>	2	0.3	0.5	0.15	0.06	0.8	7.8	
	5	1.5	0.5	0.75	0.32	3.4	9.4	
	8	3.0	0.5	1.5	0.64	7.8	8.2	
<u>Side</u>	2	0.2	0.1	0.02	0.01	0.8	1.1	<u>x 2 sides</u> 2.2
	5	1.1	0.2	0.22	0.09	3.4	2.7	5.5
	8	2.1	0.25	0.53	0.22	7.8	2.9	6.0

\* From Fig. 29

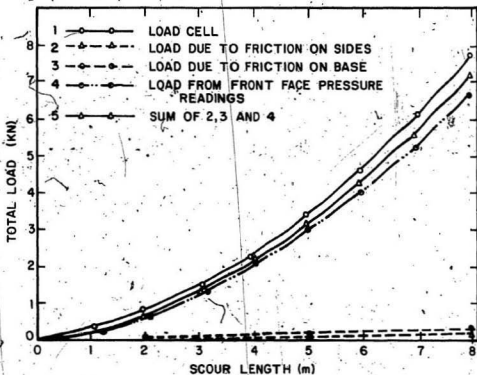


FIG. 37 COMPARISON OF THE MEASURED TOTAL SOIL RESISTANCE ON ICEBERG MODEL L1 WITH THE FRONT, SIDE AND BASE COMPONENTS OF SOIL RESISTANCE.

In the above equation if the depth of scour and the height of soil surcharge are known from a knowledge of the soil shear strength, the theoretical resistance of the front face to the scouring process may be computed.

Experiments were conducted in which  $d$  and  $h$  were measured at different points along the length of the scour track. The length of the surcharge in front ( $l_1$ ) was also measured. A typical set of results is presented in Fig. 38. From the known values of all the variables in eqn. [1] the total theoretical frontal resistance  $P$  was computed. It was shown in the previous section that the effect of soil friction on the sides and base of the model was in the order of 10%. Thus the total theoretical resistance of the iceberg model for the laboratory scour can be calculated and drawn as shown in Fig. 39.

The actual measured force on the model is also shown in Fig. 39. There is a marginal difference between the two sets of values similar to the observations made in Fig. 37 where the total measured force was compared with the sum of the individual resistance on the different faces.

In the scour tests for clay reported in the literature (Chari 1980) a similar difference between computed and measured forces was reported and the difference was in the order of 30%. Krause (1975) has reported a similar phenomenon for tests with agricultural tillage equipment in

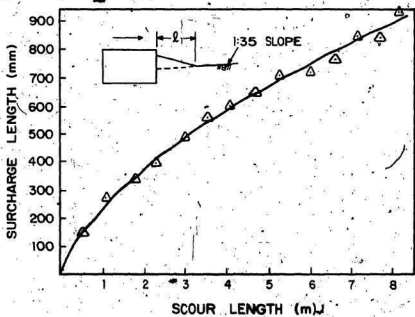
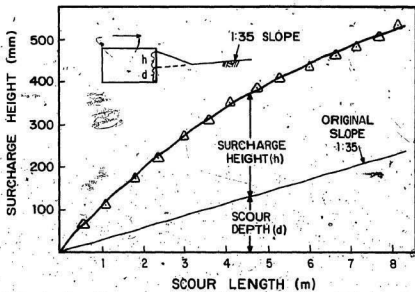


FIG. 38 MEASURED HEIGHT AND LENGTH OF SURCHARGE FOR ICEBERG MODEL 4.1

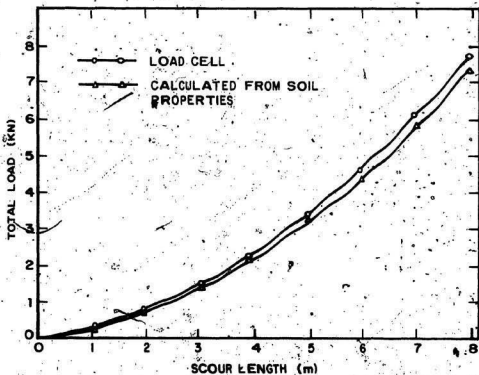


FIG. 39 COMPARISON OF MEASURED AND THEORETICAL TOTAL FORCE ON ICEBERG MODEL L1

loose sands. It was postulated by Chari (1975) that there is a movement of soil far ahead of the rupture plane. This was demonstrated by embedding pressure transducers in the soil and by measuring increases in soil pressure (Fig. 40). Based on these observations a zone of soil movement was identified (Fig. 41) as undergoing a process of local compression.

In the present series of tests the soil used is sand but the phenomenon is basically similar to that investigated by Chari (1975), Siemens (1963) and Krause (1975). It is most likely that the difference observed in Fig. 37 and 39 is due to the soil compression outside the actual zone of scour. This phenomenon is discussed further in regard to its implications and effects on pipelines buried below the maximum of iceberg scour in section 5.3 in this chapter.

There are several other variables which could influence the laboratory results and the computations. Strain rate effect in soil is an important aspect and since the iceberg is moving at a certain velocity, and the soil does not fail under static conditions it would be necessary to examine the effect of iceberg velocity on the soil resistance.

Two other aspects that would influence the results are the width of the model and the shape of the frontal scouring face of the model. These aspects are discussed in the following sections.

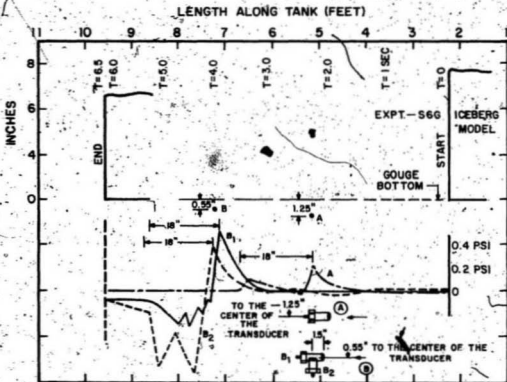


FIG. 40 RESULTS OF THE EXPERIMENT WITH PRESSURE TRANSDUCERS INSIDE THE SOIL (CHARI-1975)

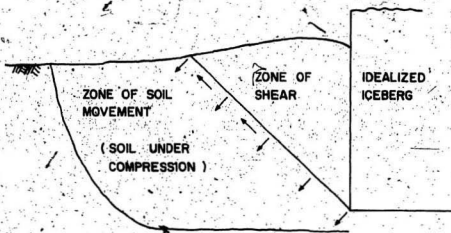


FIG. 41 CONCEPTUAL SOIL MOVEMENT IN FRONT OF THE IDEALIZED ICEBERG (CHARI 1975)

### 5.2.5 Effect of towing speed

As discussed in section 2.2.3, freely floating icebergs may achieve short term drift velocities up to 1.2 m/sec (El-Tahan et al. 1983). During the actual scouring process the velocity will gradually decrease. Thus the rate of strain of soil rupture is not constant.

The influence of speed on soil resistance has been studied by a number of researchers (Thompson 1966, Wismer and Luth 1972, Murff and Coyle 1972, 1973a). It is known that clays are more sensitive to the speed of model penetration than sands. In the earlier series of experiments with cohesive soils and the 229 mm wide models Chari (1975) reported that speeds up to 0.4 m/sec did not influence the soil resistance. It is also documented by Murff and Coyle (1972) that the velocity of penetration does not influence soil resistance in cohesionless soils up to about 10 m/sec. However, in order to examine the phenomenon in relation to the iceberg scouring, the 500 mm wide model was tested at different speeds of penetration from 0.05 to 0.20 m/sec. The upper limit of the speed was restricted by the limitations of the laboratory facilities and the speed of the motor operating the tow carriage.

Several tests were conducted and the results plotted in Fig. 42. The normal scatter that may be expected in experimental results of this type may be seen in Fig. 42.

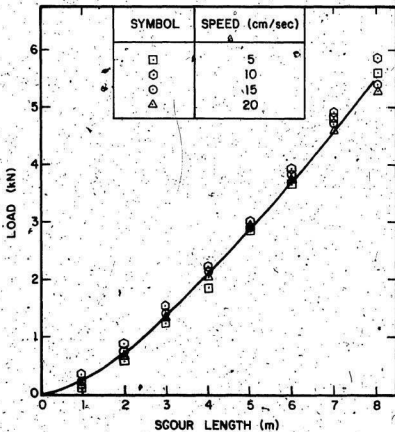


FIG. 42 EFFECT OF ICEBERG MODEL SPEED ON MEASURED LOAD FOR MODEL L1

There is no indication of any increase or decrease in soil resistance due to a variation in the speed of penetration.

Based on the reported results of similar tests in cohesionless soils for projectile penetration, it may be concluded that the variation in the iceberg scouring velocity does not influence the soil resistance.

#### 5.2.6 Influence of iceberg model size

Scale and end effects that may be associated with the physical modelling of any phenomenon have to be considered to substantiate the validity of the results. The constraints of physical modelling of the scour process are discussed in detail by Chari (1979). One of the physical constraints is the width of the model consistent with the width of the test tank.

The influence of width on soil resistance has been studied by others, primarily for the development of tillage equipment (Payne 1956, Siemens 1963). Payne (1956) used agricultural tines up to 100 mm wide in various soil types and observed a linear increase in soil resistance when the width of the towed body increased. Siemens experimented with 50 to 130 mm wide flat rectangular blades and concluded that the towing forces increased linearly as the width of the blade increased. In the present research, tests were conducted with two flat plate models L3 and S3 (Fig. 12) to

determine if the results obtained from the 500 mm model can be extrapolated to real icebergs. Model L3 was a 500 mm wide plate and model S3 was 229 mm wide.

Experiments were conducted similar to those with the prismatic model L1 and the soil resistance to models L3 and S3 were continuously measured. The soil properties and towing speed were similar to both series of tests and the results are summarized in Fig. 43. The load on model S3 was 55 to 58% lesser than the load on model L3. This is consistent with the fact model S3 was 54% narrower than model L3.

The observations from the results of these tests with the 500 and 229 mm models are in agreement with those reported by Payne (1956) and Siemens (1963) for their narrower models. Soil resistance to model penetration is directly proportional to model width and tends to increase in a linear fashion as model width increases.

#### 5.2.7 Effect of keel shape on the scour process

In practice, icebergs are of random shape and this should be accounted for in physical modelling of the scour process. Chari (1975) discussed the influence of shape on the scour process and also conducted limited tests with iceberg models having rounded and chamfered keels. It was generally concluded that while some iceberg keel shapes may,

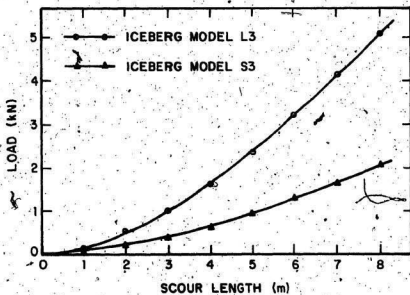


FIG. 43 COMPARISON OF LOAD MEASURED ON ICEBERG MODELS L3 AND S3.

for the purpose of analysis, be converted into an equivalent idealized shape, more research was needed in this area.

As discussed in Chapter 2 extensive data on keel shapes of icebergs have not been published in the open literature. As a first attempt at examining keel shape, the front face of the iceberg model was inclined 30° to the vertical, as shown in Fig. 12, model L2. Tests were conducted to measure the total load and front face soil pressures on this iceberg model. The results shown in Fig. 44 compare the average load measured on models L1 and L2. Inclining of the keel increased the force required to tow the model through the soil slope. The curves of Fig. 44 are summaries of average load measured in six separate tests with each model. The measured load on the inclined front face model was 15 to 35% greater than the force on a model with a vertical front face. Also there was a noticeable increase in soil pressure on the front face as shown by Fig. 45. Preliminary measurements of soil pressure on the base of iceberg model L2 also indicated slightly greater pressures than that on the model L1.

Payne and Tanner (1959) conducted field studies to examine the effect of what they refer to as "rake angle" on the performance of tillage tools. The term "rake angle" refers to the inclination of the front face of the cutting tool. They concluded rake angle was very important in

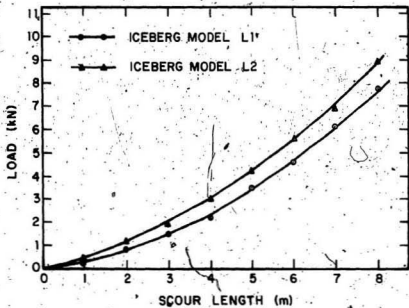


FIG. 44 COMPARISON OF LOAD MEASURED ON ICEBERG MODELS L1 AND L2

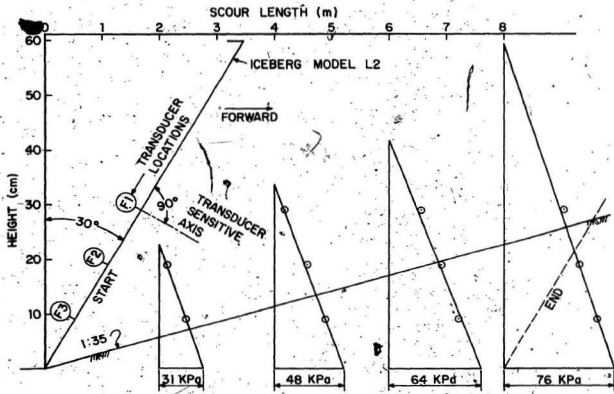


FIG. 45 VARIATION OF SOIL PRESSURE ON THE FRONT FACE OF MODEL L2

determining the type of soil displacement and also in determining the magnitude and orientation of resultant forces acting on the blade.

The preliminary tests to examine keel shape that were completed for this research and the work of others (Chari 1975, Payne and Tanner 1959) reflect the significance of keel shape in the scour process. Besides affecting the forces required to scour the soil and the local soil deformations adjacent to the scour boundary, the keel shape has implications for soil pressures in the soil at depths below the maximum scour incision. This particular aspect of soil pressures below the iceberg during the scour process is discussed in the next section (5.3).

The above observations at this time are to be considered preliminary because of the limited series of tests conducted. However, it is intuitively obvious that the forces on an inclined face would be different as may be expected even for the static case of retaining walls. Experiments described above show up to a 35% increase in the total soil resistance. Under typical field conditions it may also be expected that the inclination of the front face and the increasing soil resistance in the horizontal direction may cause an uplift of the entire iceberg resulting in a shorter scour length. Any investigation using a sloping or curved front for the iceberg model should also take into

account the tendency of the iceberg to lift up. These are topics that should be investigated in future research.

The shape of the front face and the consequent uplift would also influence the soil pressure below the depth of maximum scour. This particular occurrence was briefly discussed in section 2.1. Actual experiments were conducted by embedding pressure transducers inside the soil to delineate the zone of soil movement. Results of these tests are presented and discussed below.

### 5.3 Tests on the Pipeline Model

#### 5.3.1 General

The phenomenon of soil displacement and compression outside the immediate zone of iceberg scour was identified and briefly discussed in the previous section (Fig. 41). This phenomenon was further examined in detail using an instrumented pipeline model (Fig. 18 and 19) buried in the soil at various locations relative to the scouring iceberg model. The results of those tests are presented and discussed below.

The physical features of the pipeline model, the design criteria, the instrumentation and the experimental technique were discussed in Chapter IV.

Initially it was decided to position the pipeline model at right angles to the scour track with the pressure transducers along the center of the scour. Tests were also conducted to measure the soil pressure away from the centerline of the scour track and extending laterally beyond the scour width.

Preliminary tests were conducted to establish the approximate maximum expected soil pressures on the 122 mm diameter pipe by burying it at an arbitrary location in the tank. The pipeline model was embedded 117 mm below the maximum depth of scour at the 5 m scour length (Fig. 46). Tests were completed to measure the soil pressure on the various sides of the pipe model and the results are presented in Fig. 46. The figure shows, for each of the 8 sides, a continuous recording of normal soil pressure on the pipe wall as the iceberg model scoured above. The different faces of the pipe are suitably identified in the figure. Maximum pressures were measured on faces A, B and C which comprise the upper quarter of the pipe cross section facing the approaching iceberg model. It is of interest to note that a change in pressure is felt on all the 8 sides of the pipeline model, but faces A, B and C are the critical faces subjected to an increase in soil pressure. It was therefore decided to confine all further tests to the measurement of pressure on these three critical faces.

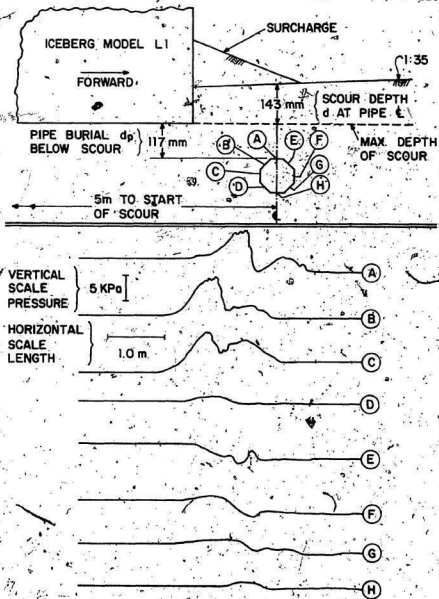


FIG. 46. COMPARISON OF SOIL PRESSURES MEASURED ON THE EIGHT SIDES OF THE PIPELINE MODEL

The experiments were conducted to determine the effect of two parameters; the depth of burial below the maximum depth of scour,  $d_p$ , and the location of the pipeline along the scour length. Figure 47 shows the location of the pipeline model for the different tests. The depth of burial below the deepest scour ranged from 10 to 121 mm at all the 3 test locations. Some limited tests were also conducted in which the pipeline model was buried inside the scour zone at the 5 m scour length point and the iceberg model was pushed into the soil bringing it as close as possible to the buried pipeline without actually hitting or gouging the pipeline model.

### 5.3.2 Results of tests on the pipeline model

The results of all the pipeline tests are summarized in Figs. 48 to 56. For the purpose of easy comparison and relative evaluation the figures are all drawn to the same scale. Comparative discussion will be made by considering the pressure variation on one face at a time for the three typical locations of the pipeline.

Figures 48, 49 and 50 show the pressures on face A when the pipeline was positioned respectively at stations 1, 2 and 3, the 2, 5 and 7 m locations of the scour track. The corresponding pressure readings on face B are given in Figures 51, 52 and 53 and finally Figs. 54, 55 and 56 show

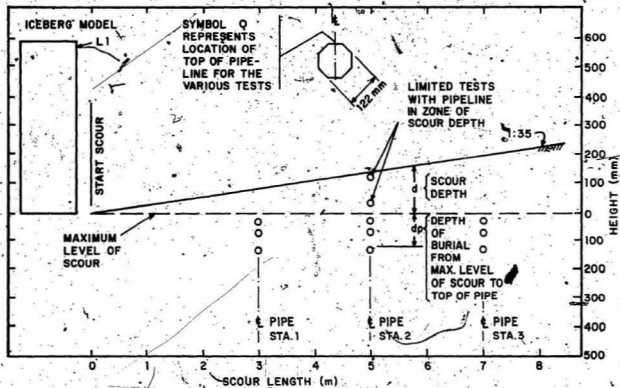


FIG. 47 LOCATIONS OF THE PIPELINE MODEL IN THE SOIL TEST BED FOR THE EXPERIMENTS WITH ICEBERG MODEL L1

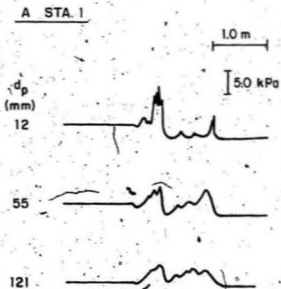
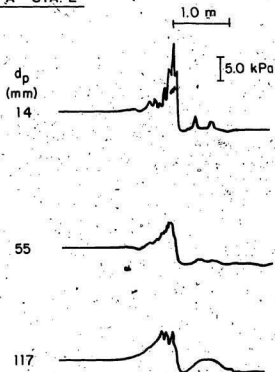


FIG. 48 PIPELINE RESULTS, MODEL L1, A, STATION 1

A STA. 2FIG. 49 PIPELINE RESULTS, MODEL L1, A<sub>p</sub> STATION 2

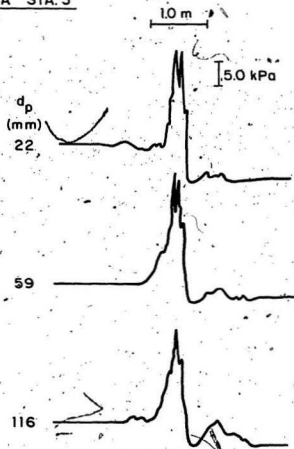
A STA. 3

FIG. 50 PIPELINE RESULTS, MODEL L1, A, STATION 3

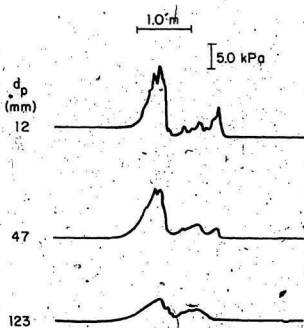
B STA. 1

FIG. 51 PIPELINE RESULTS, MODEL L1, B, STATION 1

B STA. 2

127

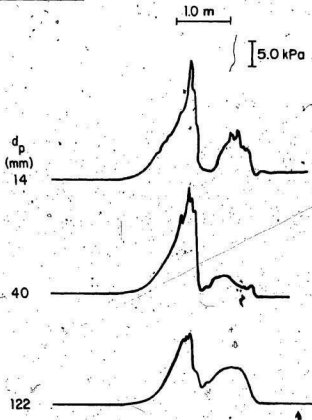


FIG. 52 PIPELINE RESULTS, MODEL L1, B, STATION 2

B STA. 3

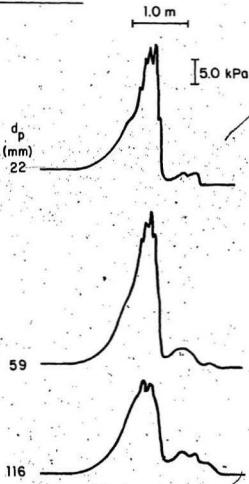


FIG. 53 PIPELINE RESULTS, MODEL L1, B, STATION 3

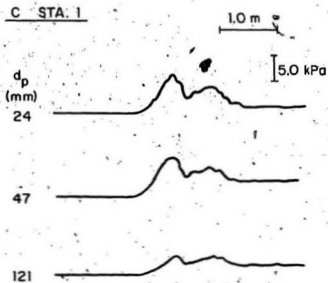


FIG. 54 PIPELINE RESULTS, MODEL L1, C, STATION 1

C STA. 2

1.0 m

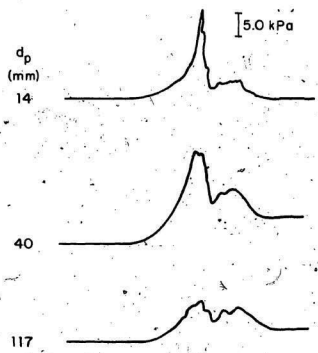


FIG. 55 PIPELINE RESULTS, MODEL L1, C, STATION 2

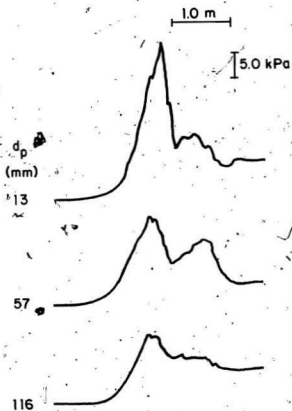
C STA. 3

FIG. 56 PIPELINE RESULTS, MODEL L1, C, STATION 3

the pressures on the face C. Inspection and comparison of the pipeline test results reveal some general patterns which are identified and discussed below.

The phenomenon of soil movement outside the scour zone was discussed qualitatively in section 5.2.4. Results of the tests with the model pipeline indicate that the influence of the scouring iceberg model extends well ahead of the front face and below the keel. The pressure transducer on face B of the pipeline model generally showed the first indication of soil movement when the iceberg model was as far away as 1.2 m from the pipeline station 3. The pressure on face B increased rapidly and reached a maximum when the leading edge of the scouring iceberg was still about 0.25 m from the center of the pipeline model. Maximum pressure on faces A and C was observed to occur when the leading edge of the iceberg model was directly above the corresponding transducer. While the pattern of soil pressure fluctuation on the pipeline model during the scouring process is of general interest, the primary concern from an engineering viewpoint is the maximum pressure exerted on the pipeline and the attenuation of this peak value with increasing depth of burial. These aspects are discussed below.

The variation of the peak pressures on faces A, B and C, with increasing depth of burial for the three pipeline locations is shown in Figs. 57, 58 and 59. It is to be noted

that these pressure variations are for the case when the transducers were directly below the centerline of the scour track. Intuitively it is to be expected that the soil pressure will decrease in the deeper zones which is clearly established by the variation in Figs. 57, 58 and 59. Further, as the depth of scour increases there is an increase in the volume of soil that is plowed, an increase in the height of the surcharge in front of the scouring iceberg and in the length of the rupture surface. Consequently there will be an increase in the magnitude of the pressures measured on faces A, B and C with increasing depth of scour and for a given level of burial below the maximum scour depth.

Theoretically, using the method of characteristics, Chari et al (1982) computed the components of the soil pressure at different points along the plane of rupture. These theoretical results were compared with the pressures measured on the pipeline model and the comparison is shown in Fig. 60. It is to be noted that the theoretical computations are for points on the plane of rupture and Fig. 60 primarily demonstrates the validity of the measurements of the pressure on the pipeline model which was buried below the depth of maximum scour. Peak pressure measurements compared with corresponding peak theoretical pressures demonstrate a decreasing soil pressure with increasing depth of burial.

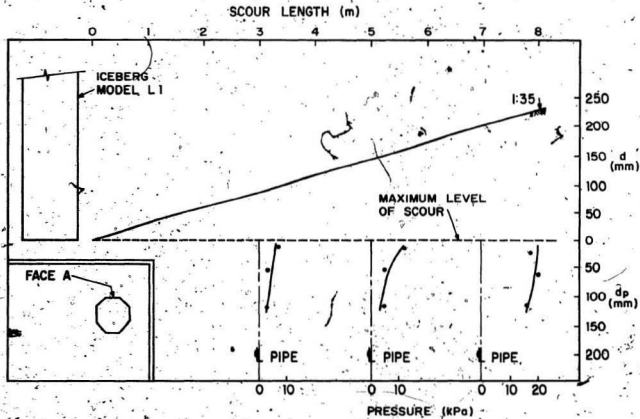


FIG. 57. MAXIMUM MEASURED PRESSURES ON FACE A OF THE PIPELINE MODEL

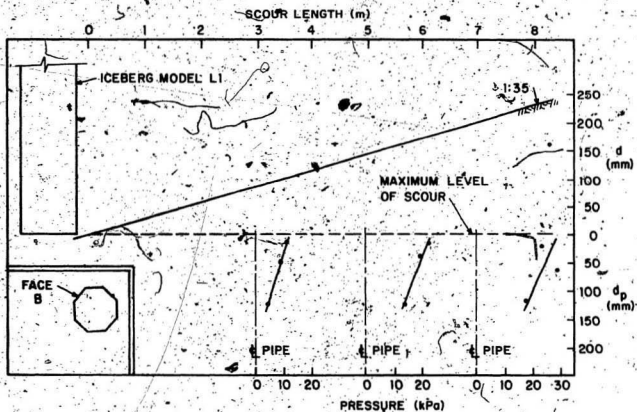


FIG. 58 MAXIMUM MEASURED PRESSURES ON FACE B OF THE PIPELINE MODEL

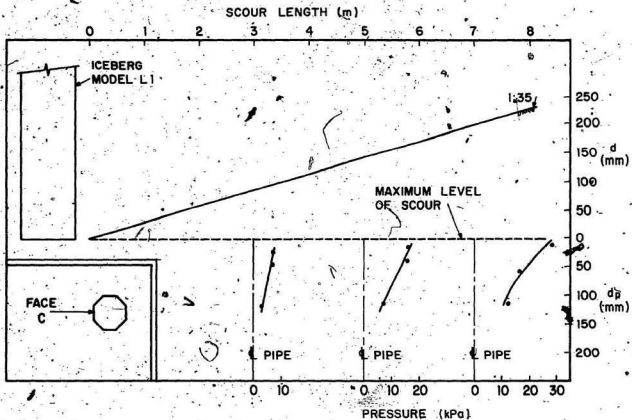


FIG. 59 MAXIMUM MEASURED PRESSURES ON FACE C OF THE PIPELINE MODEL.

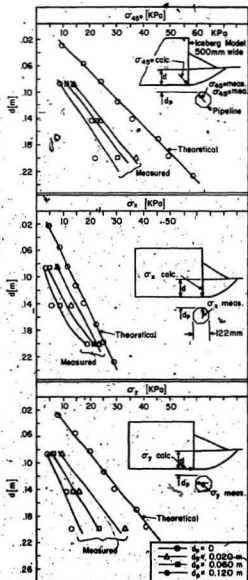


FIG. 60 COMPARISON OF THEORETICAL AND MEASURED PRESSURES (CHARI ET AL. 1982)

The relationship between the measured and theoretical pressures as a function of (the relative depth of burial (the ratio of the depth of burial to the depth of scour at that point) is shown in Fig. 61. It is seen that as the relative depth of burial increases the soil pressure drops sharply up to a relative depth of 0.5 beyond which the rate of decrease is somewhat slower. At a relative depth of 0.5 the intensity of pressure is reduced to 30 to 40% of the computed theoretical maximum pressure on the rupture surface. Based on these tests it may be preliminarily concluded that it will be desirable to bury pipelines below the mudline to a depth of 1.5 times the anticipated maximum depth of scour at any offshore location.

The above conclusions are however to be qualified. The depth of influence discussed above is very much dependent on the type of soil. The guidelines suggested above are applicable to the type of cohesionless soils used in these experiments. It is also to be noted that the physical and theoretical models discussed here are for a horizontal plowing action in which the iceberg is buoyant or nearly buoyant, however if there is a ride up of the iceberg in the process of scouring, additional pressures will be introduced due to the resultant uplifted weight. The problem then becomes one of bearing capacity combined with passive soil pressure. This is a topic for further investigation.

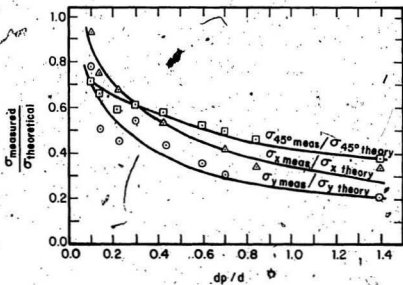


FIG. 61 REDUCTION OF PRESSURE WITH INCREASING DEPTH OF PIPELINE BURIAL BELOW THE SCOUR (CHARI ET AL. 1982)

### 5.3.3 Soil pressure away from the center line of scour

As mentioned previously, some tests were conducted to measure the soil pressure variation away from the center of the scour track. Results of these tests are presented in Fig. 62, which shows a comparison between soil pressures on the pipeline model for face B at three different locations. For the two locations in the 500 mm scour width (B1 and B2) there was only a small variation in soil pressure between the center of the scour track and near the edge of the scour. However, at a short distance outside the scour track (B3) the maximum measured pressure was approximately 35% of that measured at the center of the scour. It is a well known fact both in anchor design and in research with agricultural equipment that the passive pressure zone extends laterally to a short distance beyond which the soil virtually stays in its in situ condition. The results shown in Fig. 62 further confirm this principle.

### 5.3.4 Results of tests with the pipeline model in the scour zone

Some limited tests were conducted in which the pipeline model was embedded at a depth shallower than the depth of the iceberg model keel. However in these tests the iceberg model was stopped before it could hit the pipeline. The purpose of these tests was to delineate the zone of soil movement in front of the scouring iceberg. The entire half

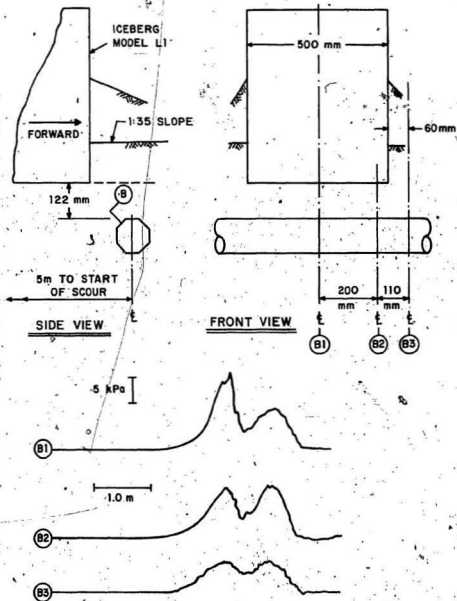


FIG. 62 PIPELINE RESULTS, MODEL L1, LATERAL VARIATION OF PRESSURE ON THE PIPE

of the pipeline model that is exposed to the scouring iceberg is subjected to pressures of different intensities as seen from Figs. 63 and 64. The intensity of pressure at any point would be dependent on the locations of the pipeline model with respect to the iceberg keel. It may be seen that there is a movement of soil as far away as one meter as recorded by the pressure transducers and shown in Figs. 63 and 64.

#### 5.3.5 Effect of iceberg keel shape on results of the pipeline tests.

The effect of iceberg keel shape on the maximum scour depth was discussed in section 5.2.7. Some limited tests were conducted with the iceberg model L2 in which the pipeline model was buried below the maximum depth of iceberg scour and the pressures on the different faces were measured similar to the experiments with model L1.

From the results shown in Figs. 44 and 45 it was concluded that the soil resistance increases when the front face of the iceberg model was inclined. Figure 65 shows the pressure on face B for the test with model L2. The figure also shows a comparison with the results of the tests with model L1. The inclined keel results in a soil pressure which is 30% higher. This is consistent with similar differences of total force measured on iceberg model L1 and L2. Further theoretical and experimental work on this aspect is suggested.

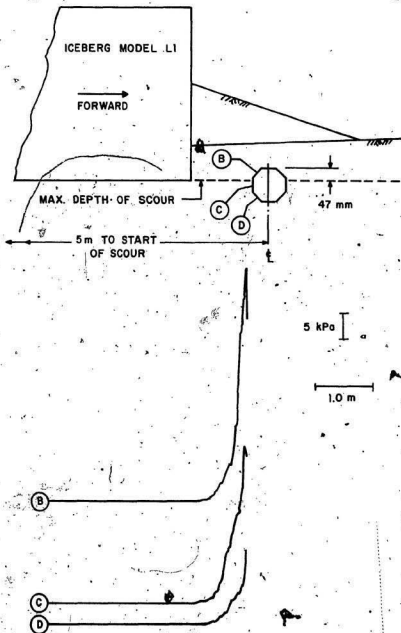


FIG. 63 PIPELINE RESULTS, MODEL L1, TOP OF PIPE 47 mm ABOVE MAXIMUM DEPTH OF SCOUR

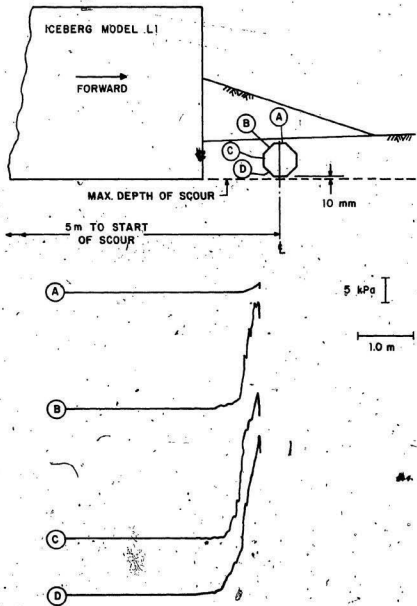


FIG. 64 PIPELINE RESULTS, MODEL L1, TOP OF PIPE 132 mm ABOVE MAXIMUM DEPTH OF SCOUR

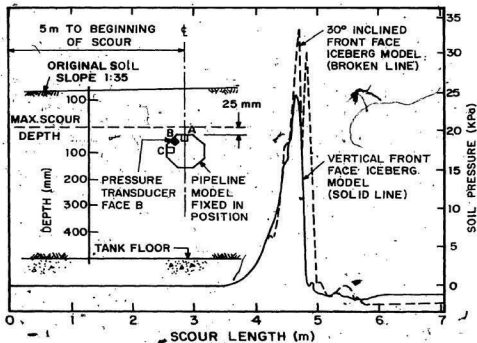


FIG. 65 COMPARISON OF PRESSURE ON THE PIPELINE MODEL FOR ICEBERG MODEL'S L1 AND L2

## CHAPTER VI

## SUMMARY AND CONCLUSIONS

The research completed for the purpose of this study was primarily an experimental approach to examine the geotechnical aspects of the iceberg scour phenomenon. The experimental program consisted of qualitative observations and quantitative tests and measurements. The iceberg scour process was physically modelled in the laboratory using 500 mm wide instrumented iceberg models and a cohesionless sand as the seafloor soil. A method of soil test bed preparation to obtain repeatability of the test sample was determined for the 14 m long x 3 m wide x 1 m deep towing tank facility. The applicability of the theoretical iceberg scour equations was verified by conducting tests with prismatic models and plates of two different sizes. The influence of the scouring iceberg below the maximum scour depth was examined using an instrumented pipeline model which was embedded at various locations relative to the incision depth. The salient observations and conclusions from the research are as follows:

1. Laboratory tests clearly show that field scours are not likely to retain their original form and may

be obliterated due to several environmental factors. The original maximum scour depth may be obscured in course of time, depending on the shape and width of the iceberg keel, the depth of the scour, the natural slope angle of the soil and the dynamics of the seafloor.

2. The primary resistance to scour for the horizontal plowing action of an iceberg is the passive soil pressure developed on the front face of the iceberg keel. The mechanism of soil failure in front of the advancing iceberg model will be characterized by a series of successive failure planes.

3. The friction component of soil resistance on the sides and base for the scouring iceberg model in a frictional soil is not significant compared to the total soil resistance. Preliminary calculations indicate that ignoring friction effects in cohesionless soils may result in a marginal overestimation of scour depth in the order of 10%.

4. The theoretical computation of soil resistance on the iceberg model is about 10% less than the measured soil resistance. This is attributed to a process of soil compression both ahead of and below the scouring iceberg keel which is not accounted for in theoretical calculations.

5. The velocity of an iceberg during scouring

does not influence the soil resistance as there is no strain rate effect in the range of velocities common to icebergs.

6. Scale and end effects were not detected in these tests based on the evidence of two different widths of models, 229 and 500 mm. Soil resistance was noted to be directly proportional to model width.

7. The shape of the iceberg keel was determined to be an important factor affecting soil resistance during the scour process. Inclination of the keel by 30° caused as much as a 35% increase in soil resistance.

8. Pipelines buried even below the depth of maximum iceberg scour will be subjected to soil movement caused by the scouring process. The critical area of the pipeline subjected to maximum pressure is the upper quarter of the pipeline facing the iceberg.

9. The pressure on the buried pipeline decreases with increasing depth of burial below the scour and with distance from the center of the scour track.

Based on the experiments completed, it is felt that several aspects of the iceberg scour modelling require further research:

1. Additional theoretical work is recommended to examine the influences of iceberg keel shape, and seabed soil type. The resulting forces on the soil for various

combinations of keel shape and sediment type should be considered particularly as they relate to overburden pressures in the soil beneath the maximum scour depth.

2. Further physical modelling is suggested in which uplift and tilting of the iceberg model is permitted and measured. It is also recommended that further work be done on the zone of influence of soil pressure for an uplifted berg.

3. A comprehensive study is recommended to collect and correlate existing field data related to scour sizes, soil type and iceberg dimensions and to compare these with the theoretical computations.

BIBLIOGRAPHY

1. ABDELNOUR, R., LAPP, D., HAIDER, S., SHINDE, S.B., WRIGHT, B. (1981) Model Tests of Sea Bottom Scouring, in Proceedings of PQAC 81, Vol. 2, pp. 688-705.
2. ARCTIC PETROLEUM OPERATORS ASSOCIATION (APOA) (1975) An Analytical Study of Ice Scour on the Sea Bottom, APOA 69-1, report by FENCO Ltd.
3. ALLAIRE, P.E. (1972) Stability of Simply Shaped Icebergs, Journal of Canadian Petroleum Technology, Vol. 11, No. 4, pp. 21-25.
4. ALLEN, J. (1971) An Analysis of the Effect of Bottom Scouring Icebergs, in Proceedings of the Canadian Seminar on Icebergs, Under Auspices of Maritime Command Canadian Forces, Halifax, N.S., Dec. 6-7.
5. AMOS, C.L. and BARRIE, J.V. (1980) Hibernia and Ben Nevis Seabed Study, Polaris V Cruise Report June 1980, C-CORE Data Report No. 80-17, October 40 p.
6. AROCKIASAMY, M., EL-TAHAN, H., SWAMIDAS, A.S.J., RUSSEL, W., REDDY, D.V. (1983) Semi-Submersible Response to Bergy-Bit Impact, in Preprints of the International Symposium on Semi-Submersibles: The New Generation, Mar. 17-18, London, England, 22 p.
7. BARNES, P.W., REIMNITZ, E., REARIC, D.M. (1982) Ice Gouge Characteristics Related to Sea-Ice Zonation, Beaufort Sea, Alaska, in Preprints NRCC Ice Scour Workshop, Montebello, Quebec, 32 p.
8. BARRIE, J.V., WOODWORTH-LYNAS, C.M.T., GIDNEY (1982) Iceberg Grounding Review from Wellsite Observations, C-CORE Report No. 82-7, 38 p.
9. BARSVARY, A.K., KLYM, T.W. and FRANKLIN, J.A. (1980) List of Terms, Symbols and Recommended SI Units and Multiples for Geotechnical Engineering, Canadian Geotechnical Journal, Vol. 17, pp. 89-96.
10. BENEDICT, C.P. (1976) Icebergs and Canadian East Coast Exploration, the 31st Annual Petroleum Mechanical Engineering Conference, Mexico City, Mexico, September.

11. BOWLES, J.E. (1982) Foundation Analysis and Design, McGraw-Hill, Third Edition, 816 p.
12. CARSOLO, A.J. (1954) Microrelief on Arctic Seafloor, in Bulletin of the American Association of Petroleum Geologists, Vol. 38, No. 7, pp. 1587-1601.
13. CHARI, T.R. (1975) Some Geotechnical Aspects of Iceberg Grounding, Ph.D. Thesis, Memorial University of Newfoundland, St. John's, Newfoundland, 181 p.
14. CHARI, T.R. (1979) Geotechnical Aspects of Iceberg Scours on Ocean Floors, Canadian Geotechnical Journal, Vol. 16; No. 2, pp. 379-390.
15. CHARI, T.R. (1980) A Model Study of Iceberg Scouring in the North Atlantic, Journal of Petroleum Technology, December, pp. 2247-2252.
16. CHARI, T.R. and ALLEN, J.H. (1972) Iceberg Grounding - A Preliminary Theory, Applications of Solid Mechanics, Proceedings of the Symposium held at the University of Waterloo, June, 1972, (S.M. Study No. 7), pp. 81-95.
17. CHARI, T.R. and ALLEN, J.H. (1974) An Analytical Model and Laboratory Tests on Iceberg Sediment Interaction, Proceedings I.E.E.E., Vol. 1, pp. 133-136.
18. CHARI, T.R. and GREEN, H.P. (1981) Iceberg Scour Studies in Medium Dense Sands, in Proceedings of POAC 81, Vol. 2, pp. 1012-1019.
19. CHARI, T.R., GREEN, H.P. and REDDY, A.S. (1982) Some Geotechnical Aspects of Iceberg Furrows, in Preprints Second Canadian Conference on Marine Geotechnical Engineering, Halifax, Nova Scotia, 4 p.
20. CHARI, T.R. and GUHA, S.N. (1978) A Model Study of Iceberg Scouring in North Atlantic, in Proceedings of OTC 78, Vol. 3, pp. 2319-2326.
21. CHARI, T.R., HODDINOTT, T.K. and GREEN, H.P. (1983) Geotechnical Report on Piston Cores from Davis Strait, Report Prepared for C-CORE.

22. CHARI, T.R. and MUTHUKRISHNAIAH, K. (1978) Model Studies of Ocean Floor Scouring by Icebergs, in Proceedings of the Speciality Conference on Applied Techniques for Cold Environments, ASCE, pp. 828-839.
23. CHARI, T.R., PETERS, G.R. and MUTHUKRISHNAIAH, K. (1980) Environmental Factors Affecting Iceberg Scour Estimates, Cold Region Science and Technology, Vol. 1, pp. 223-230.
24. CHARI, T.R. and PETERS, G.R. (1981) Estimates of Iceberg Scour Depths, in Proceedings of the Symposium on Production and Transportation Systems for the Hibernia Discovery, St. John's, Newfoundland, Feb., pp. 178-188.
25. DINSMORE, R.P. (1972) Ice and its Drift into the North Atlantic Ocean, Symposium on Environmental Conditions in the Northwest Atlantic, 1960-1969, ICNAF Special Publication No. 8, pp. 89-128.
26. DREDGE, L.A. (1982) Relict Ice-Scour Marks and Late Phases of Lake Agassiz in Northernmost Manitoba, Canadian Journal of Earth Sciences, Vol. 19, pp. 1079-1087.
27. ESRIG, M.I. and KIRBY, R.C. (1977) Implications of Gas Content for Predicting the Stability of Submarine Slopes, Marine Geotechnology, Vol. 2, pp. 81-100.
28. EL-TAHAN, H., EL-TAHAN, M., VENKATISH, S. (1983) Forecast of Iceberg Ensemble Drift, in Proceedings of OTC 83, Vol. 1, pp. 151-158.
29. EL-TAHAN, M.S. (1980) Modelling of Iceberg Drift, M.Eng. Thesis, Memorial University of Newfoundland, St. John's, Newfoundland, 72 p.
30. EMBLETON, C. and KING, C.A.M. (1971) Glacial and Periglacial Geomorphology, Edward Arnold Publishing Limited, London, England, 608 p.
31. FADER, G.B. and KING, L.H. (1981) A Reconnaissance Study of the Surficial Geology of the Grand Banks of Newfoundland, in Current Research Part A, Geological Survey of Canada, Paper 81-1A, pp. 45-81.

32. FILLON, R.H. and HARMES, R.A. (1982) Northern Labrador Shelf Glacial Chronology and Depositional Environments, Canadian Journal of Earth Sciences, Vol. 19, No. 1, pp. 162-192.
33. <sup>SE</sup> GEOCON LIMITED (1969) Soil Sampling - Grand Bank 1969 report prepared by Geocon Limited, Rexdale, Ontario for Amoco Canada Petroleum Company Limited, Calgary, Alberta.
34. GEOCON OFFSHORE (1980) Marine Geotechnical Investigations, Hibernia and Ben Nevis Areas Grand Bank Newfoundland, reports prepared for Geocon Offshore, Toronto, Ontario for Mobil Oil Canada Limited, Calgary, (reviewed by author with permission of C-CORE).
35. GRAHAM, B.W., NIXON, J.F. (1979) Some Geotechnical Properties of Seabed Samples from Davis Strait, Northwest Territories, in Proceedings of the First Canadian Conference on Marine Geotechnical Engineering, pp. 290-300.
36. GRANT, A.C. (1972) The Continental Margin Off Labrador and Eastern Newfoundland - Morphology and Geology, Canadian Journal of Earth Sciences, Vol. 9, pp. 1394-1430.
37. GREEN, H.P. and CHARI, T.R. (1981) Sediment Compaction Below Iceberg Furrows, Conference Record Oceans '81, IEEE-MTS Conference, Vol. 1, pp. 223-227.
38. GREEN, H.P., REDDY, A.S. and CHARI, T.R. (1983) Iceberg Scouring and Pipeline Burial Depths, in Proceedings of POAC '83, Vol. 1, pp. 280-288.
39. GREEN, H.W., MEULEMAN, A.W., DESSUREAULT, M.J. (1982) Trenching Across the Strait of Belle Isle - Marine Geotechnical Investigations, paper presented at the Second Canadian Conference on Marine Geotechnical Engineering, Halifax, Nova Scotia, 12 p.
40. GUSTAJTIS, K.A. (1979) Iceberg Scouring on the Labrador Shelf Saglek Bank, C-CORE Technical Report No. 79-13, 89 p.
41. HARRIS, I. McK. (1974) Iceberg Marks on the Labrador Shelf, Geological Survey of Canada, Paper 74-30, pp. 97-101.

42. HARRIS, I. McK. and JOLLYMORE, P.G. (1974) Iceberg Furrow Marks on the Continental Shelf Northeast of Belle Isle, Newfoundland, Canadian Journal of Earth Sciences, Vol. 2, No. 1, pp. 43-52.
43. HOVLAND, M. (1983) Elongated Depressions Associated with Pockmarks in the Western Slope of the Norwegian Trench, Marine Geology, Vol. 51, pp. 35-46.
44. JOSENHANS, H.W. (1983). Evidence of Pre-Late Wisconsinan Glaciations on Labrador Shelf - Cartwright Saddle, Canadian Journal of Earth Sciences, Vol. 20, pp. 225-235.
45. JOSENHANS, H.W. and BARRIE, J.V. (1982) Preliminary Results of Submersible Observations on the Labrador Shelf, in Current Research Part B, Geological Survey of Canada, Paper 82-1B, pp. 269-276.
46. KELLOR, G.H. (1969) Engineering Properties of Some Seafloor Deposits, Journal of Soil Mechanics and Foundations Division, ASCE, Vol. 95, No. SM6, pp. 1379-1392.
47. KING, L.H. (1976) Relict Iceberg Furrows on the Laurentian Channel and Western Grand Banks, Canadian Journal of Earth Sciences, Vol. 13, pp. 1082-1092.
48. KIVISILD, H.R. (1981) Use of Mathematical Models to Estimate Ice Scour, paper presented at the Conference on Canadian Offshore Drilling and Downhole Technology, Edmonton, Alberta, 9 p.
49. KIVISILD, H.R. (1982) The Influence of Soil Properties on Scour, paper presented at the Second Canadian Conference on Marine Geotechnical Engineering, Halifax, Nova Scotia, June, 7 p.
50. KIVISILD, H.R., PILKINGTON, G.R. and IYER, S.H. (1981) Mathematical Analysis of Ice Scour, American Society of Mechanical Engineers, Energy Sources Technology Conference, Jan. 18-21, 1981, Houston, Texas, 16 p.
51. KOLLMEYER, R.C. (1980) West Greenland Outlet Glaciers: An Inventory of the Major Iceberg Producers, Cold Regions Science and Technology, Vol. 1, pp. 175-181.
52. KOVACS, A. (1972) Ice Scouring Marks Floor of the Arctic Shelf, Oil and Gas Journal, October 23.

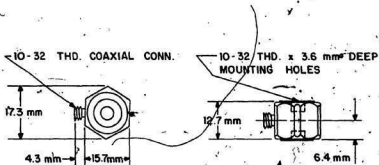
53. KRAUSE, R. (1975) The Most Important Phenomenon Subsoiling in Dry Sand, Journal of Terramechanics, Vol. 12, No. 3/4, pp. 119-130.
54. LEWIS, C.F.M. (1981) Report on Cruise BIO No. 81-012 CSS Baffin, Bedford Institute of Oceanography, Dartmouth, Nova Scotia, 24 p.
55. LEWIS, C.F.M. and BARRIE, J.V. (1981) Geological Evidence of Iceberg Groundings and Related Seafloor Processes in the Hibernia Discovery Area of Grand Bank, Newfoundland, in Proceedings of the Symposium on Production and Transportation Systems for the Hibernia Discovery, St. John's, Newfoundland, pp. 146-177.
56. LEWIS, C.F.M., MACLEAN, B. and PALCONER, R.K.H. (1979) Iceberg Scour Abundance in Labrador Sea and Baffin Bay: A Reconnaissance of Regional Variability, in Proceedings of the First Canadian Conference on Marine Geotechnical Engineering, pp. 79-94.
57. LITVIN, V.M. and RVACHEV, V.D. (1963) The Bottom Topography and Sediments of the Labrador and Newfoundland Fishing Areas, in Soviet Fisheries Investigations in the Northwest Atlantic, Polar Scientific - Research Institute of Marine Fisheries and Oceanography, Moscow, U.S.S.R. (1962), pp. 100-112. Translation published by the National Science Foundation, Washington, D.C. in Jerusalem, Israel.
58. MACLAREN ATLANTIC LIMITED. (1976) Report on Sediment Analysis of Cores from Davis Strait and Flemish Pass, report to Imperial Oil Limited.
59. MILNE, A.R. (1973) Methods for Launch and Recovery of Sea Bottom Instrument Package, Underwater Journal, October, pp. 213-220.
60. MCCLELLAND ENGINEERS (1971) Soil Borings - Grand Bank 1971, Report Prepared by McClelland Engineers, Houston, Texas for Amoco Canada Petroleum Company Limited, Calgary, Alberta.
61. MOUNTAIN, D.G. (1980) On Predicting Iceberg Drift, Cold Regions Science and Technology, Vol. 1, pp. 273-282.

62. MUDIE, P.J. and GUILBAULT, J.P. (1982) Ecostratigraphic and Paleomagnetic Studies of Late Quaternary Sediments on the Northeast Newfoundland Shelf, in Current Research Part B, Paper 82-1B, Geological Survey of Canada, pp. 107-116.
63. MURFF, J. D., AND COYLE, H. M. (1972) A laboratory investigation of low velocity penetration. Proceedings of conference on Rapid Penetration Terr. Materials, Texas A & M University, Texas, pp. 319-359.
64. (1973a) Low velocity penetration of kaoline clay, Journal of Soil Mechanics Foundation Division, ASCE, Vol. 99, No. SM5, pp. 375-389.
65. MURRAY, J.E. (1969) The Drift, Deterioration and Distribution of Icebergs in the North Atlantic Ocean, Ice Seminar, Canadian Institute of Mining and Metallurgy, Special Vol. 10, pp. 3-18.
66. NATIONAL RESEARCH COUNCIL OF CANADA (1982) Workshop on Ice Scours, held at Montebello, Quebec.
67. NAVIGATION REPORT OF CABLE REPAIR VESSEL C.S. LORD KELVIN APRIL 17, 1961, Repair to TAT-2 East West Cable, Copy Available at C-CORE, MUN, St. John's, Newfoundland (OEIC Reference No. 801537).
68. NEUMANN, G. PIERSON, W.J. JR. (1966) Principles of Physical Oceanography, published by Prentice-Hall Inc., 545 p.
69. PAYNE, P.C.J. (1956) The Relationship Between the Mechanical Properties of Soil and the Performance of Simple Cultivation Implements, Journal of Agricultural Engineering Research, Vol. 1, No. 1, pp. 23-50.
70. PAYNE, P.C.J.; TANNER, D.W. (1959) The Relationship Between Rake Angle and the Performance of Simple Cultivation Implements, Journal of Agricultural Engineering Research, Vol. 4, No. 4, pp. 312-325.
71. PETERS, G.R. (1979) Sea ice and Icebergs in Proceedings of, POAC '79, Vol. 3, pp. 41-59.
72. ROBE, R.O., MAIER, D.C. and RUSSEL, W.E. (1980) Long Term Drift of Icebergs in Baffin Bay and the Labrador Sea, Cold Region Science and Technology, Vol. 1, pp. 183-193.

73. SIEMENS, J.C. (1963) Mechanics of Soil Under the Influence of Model Tillage Tools, Ph.D. Thesis, University of Illinois at Urbana, 139 p.
74. SLATT, R.M. (1974) Continental Shelf Sediments Off Eastern Newfoundland: A Preliminary Investigation, Canadian Journal of Earth Sciences, Vol. 11, No. 3, pp. 362-368.
75. SMITH, E.H. (1931) The Marion Expedition to Davis Strait and Baffin Bay, U.S. Coast Guard Bulletin, No. 19, Part 3, Scientific Results, pp. 60-216.
76. THOMPSON, L. J. (1966) Dynamic Penetration of Selected Projectile into Particulate Media, Sandia Lab. Rep. SC-R-R-66-376, Albuquerque, New Mexico.
77. U.S. COAST GUARD (1978) Report of the International Ice Patrol Service in the North Atlantic Ocean, Bulletin No. 64, Department of Transportation, United States Coast Guard, CG-188-33.
78. VAN der LINDEN, W.J., PILLON, R.H. and MONAHAN, D. (1976) Hamilton Bank, Labrador Margin: Origin and Evolution of a Glaciated Shelf, Marine Sciences Paper 14, 31 p.
79. WILSON, J. and FRANKLIN, R.N. (1971) Further Measurements of Drag on Bodies Moving Through Sand, Journal of Terramechanics, Vol. 8, No. 2, pp. 39-48.
80. WISMER, R.D. and LUTH, H.J. (1972) Rate Effects in Soil Cutting, Journal of Terramechanics, Vol. 8, No. 3, pp. 11-21.
81. WOODWORTH-LYNAS, C.M.T. (1983) The Relative Age of Ice Scours Using Cross-Cutting Relationships, C-CORE Technical Report No. 83-3, 53 p.

## APPENDIX A

Specifications and Calibration Procedures  
for the Load and Pressure Sensors



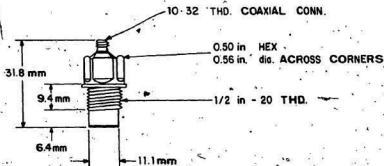
### LOAD CELL

SCALE: FULL SIZE

Kistler Model 912 Quartz Dynamic Load Cell

#### Specifications:

Range: compression	5000 lbs (2268 kg)
Resolution	0.002 lb (0.9 gm)
Overload	20%
Sensitivity (nominal)	50 pcb/lb (110 pcb/kg)
Resonant frequency (nominal) (no load)	70,000 Hz
Rigidity	$20 \times 10^{-8}$ in/lb ( $1 \times 10^{-8}$ m/kg)
Rise time	5 microsec
Linearity (zero based best straight line)	$\pm 1\%$
Capacitance (nominal)	58 picofarads
Insulation resistance (minimum)	$10^{13}$ ohms
Temperature sensitivity	0.01% per °F
Temperature range	-400° to 300°F
Side force (maximum)	100 lbs (45 kg)
Shock and vibration	10,000 g
Cable connector, side coaxial, teflon insulation	10/32 thread
Case materials	416 SS, 17-4PH SS
Weight	0.6 oz (17 gm)

**PRESSURE TRANSDUCER**

SCALE : FULL SIZE

**Kistler Model 606A/606L Quartz Pressure Transducer****Specifications:****606A\***

Range full scale	3000 psi (21 MPa)
Resolution	0.005 psi (0.03 KPa)
Maximum pressure	5000 psi (34 MPa)
Sensitivity (nominal)	5.5 pcb/psi (0.8pcb/KPa)
Resonant frequency (nominal)	130 kHz
Rise time	3.0 microsec
Linearity (zero based best straight line)	± 1%
Capacitance (nominal)	50 picofarads
Insulation resistance	10 <sup>13</sup> ohms
Acceleration sensitivity	<0.005 psi/g (0.03KPa/g)
Temperature effect on sensitivity	<0.03% per °F
Temperature range	-350° to +450° F
Shock, 1 ms pulse width	1000 g
Case material	SS
Weight	0.5 oz (14gm)

\*Model 606L is identical to 606A except for range of 30 psi and max. pressure of 300 psi  
 30 psi equals approximately 207 KPa  
 300 psi equals approximately 2068 KPa

## Calibration Procedures

The general procedure was to test the complete instrumentation system (Fig. 20) using a known input. A control pressure and load in the same range as those expected for the experiments was used. Amplifier and recorder settings and signal cable lengths and type were the same as for the experiments. For the load cells, verification of the system output was achieved by using a Instron testing machine to apply a compression load directly to the sensing axis of the load cell. A stepped-increase load of 0 to 5 kN was applied over 100 sec to simulate experiment conditions. For the pressure transducers a piston activated oil pressure chamber was constructed capable of accepting four transducers. The pressure chamber was set in a loading frame and a ramp load of 0 to 100 kPa was applied over about 100 sec. In all cases good agreement was observed between the input and output signals.

The crossface sensitivity of the pressure transducers was also examined. This was completed to verify that the soil pressures recorded during the actual scour tests were in fact due only to the normal pressures exerted by the soil on the model and not influenced by the sliding action of the transducer face against the soil. This was investigated by two methods: Comparative scour tests were

conducted with pressure transducers flush mounted with the face of the iceberg model and with pressure transducers recessed approximately 4 mm. The recessed transducers had the sensing face covered by a thin layer of steel filings taped in place which filled up the 4 mm gap thereby ensuring only forces perpendicular to the transducer would be detected by the sensor. No noticeable variation of results was observed between the flush mounted and recessed transducers. Also tests were conducted in a specially designed 200 mm shear box in which a pressure transducer was mounted in a plate in the stationary lower half of the box. The upper half of the box was filled with sand, a normal load applied and then a tangential load was applied pulling the top half of the shear box (filled with sand) across the transducer face. Again no noticeable variation in pressure transducer output was detected during the time when the normal load was applied until the top half of the shear box had travelled its limit of 75 mm (approximately 30 seconds).

## APPENDIX B

Typical Data Sheets for a Scour Experiment

## ICEBERG SCOUR TESTS

SHEET #1

TITLE \_\_\_\_\_ Tape \_\_\_\_\_ Exp. # \_\_\_\_\_  
 \_\_\_\_\_ Initial Ft. \_\_\_\_\_ Date \_\_\_\_\_  
 \_\_\_\_\_ Final Ft. \_\_\_\_\_

Ch. #	Cal. In	Cal. Out	Description	S/N	Position	Amplifier.	
						R.S.	R.M.
1							
2							
3							
4							
5							
6							
7							

Distance (m)      Voltage (v)

End of model motion \_\_\_\_\_

Start of scour \_\_\_\_\_

Start of model motion \_\_\_\_\_

Scour length \_\_\_\_\_

Iceberg model \_\_\_\_\_ width \_\_\_\_\_ length \_\_\_\_\_

ProfileFront view

## ICEBERG SCOUR TESTS

SHEET #2

Time of raking \_\_\_\_\_ Exp. # \_\_\_\_\_

Time of testing \_\_\_\_\_ Date \_\_\_\_\_

Temperature (air) \_\_\_\_\_ (soil) \_\_\_\_\_

Soil type \_\_\_\_\_ Slope \_\_\_\_\_ Depth of soil  
below model \_\_\_\_\_Thin wall cylinder density tests

Loc. #	Bowl	Tare Wt. g	Soil+ Tare g	Soil g	Vol. of Soil cm <sup>3</sup>	Density kg/m <sup>3</sup>	Depth of Sample Below Surface

PenetrometerWater ContentComments







